References for the GEISA 2015 sub-database on line transition parameters

Details of changes since the 2011 edition of GEISA

GEISA 2015 molecule numbering				
1. h2o 2. co2 3. o3 4. n2o 5. co 6. ch4 7. o2 8. no 9. so2 10. no2	11. nh3 12. ph3 13. hno3 14. oh 15. hf 16. hcl 17. hbr 18. hi 19. clo 20. ocs	21. h2co 22. c2h6 23. ch3d 24. c2h2 25. c2h4 26. geh4 27. hcn 28. c3h8 29. c2n2 30. c4h2	31. hc3n 32. hocl 33. n2 34. ch3cl 35. h2o2 36. h2s 37. hcooh 38. cof2 39. sf6 40. c3h4	41. ho2 42. clono2 43. ch3br 44. ch3oh 45. no+ 46. hnc 47. c6h6 48. c2hd 49. cf4 50. ch3cn 51. hdo 52. so3

Full details on GEISA-2015 updates are given in, Jacquinet-Husson et al., The 2015 edition of the GEISA spectroscopic database, JMS 327 (2016) 31–72, http://dx.doi.org/10.1016/j.jms.2016.06.007.

For information on non updated molecules in this 2015 edition, please refer to the article: Jacquinet-Husson et al, The 2009 edition of the GEISA spectroscopic database, JQSRT, 112 (2011) 2395–2445, http://dx.doi.org/10.1016/j.jqsrt.2011.06.004.

H_2O (molecule 1)

H_2O is significantly updated in this 2015 edition of GEISA, with important additions across the whole spectral range (67,789 lines in GEISA-2011 have become 191,846 in GEISA-2015). This significant increase of the total number of transitions originates mainly in the inclusion of empirical lists in GEISA-2015.

The new line lists for H_2O in this 2015 edition of GEISA originate from results of 8 participating institutions (in alphabetic order):

- V.E. Zuev Institute of Atmospheric Optics, Russian Federation (IAO)
- Karlsruhe Institute of Technology, Germany (KIT)
- Laboratoire Inter-Universitaire des Systèmes Atmosphériques, France (LISA)
- Laboratoire Interdisciplinaire de Physique, France (LIPhy)

- Netherlands Institute for Space Research, Netherlands (SRON)
- University College Cork, Ireland (UCC)
- University College London, UK (UCL)
- University of Massachusetts, USA (UMASS)

Five isotopologues, *i.e.*, $H_2{}^{16}O$, $H_2{}^{17}O$, $H_2{}^{18}O$, $D_2{}^{16}O$, $D_2{}^{18}O$, are present in the 2015 release, and two new isotopologues $D_2{}^{16}O$ and $D_2{}^{18}O$, are now implemented, as summarized in Table1. This Table lists GEISA-2015 172,680 entries that have totally replaced entries of GEISA-2011. Their names are listed in the first column with associated identification codes. Each line list spectral range, minimum and maximum wave numbers (cm^{-1}), the number of transitions, the mean (Moy.I) and the maximum (Max.I) of the line intensities (cm $molecule^{-1}$ at 296 K), and the origin of the data are given in columns 2 to 7 of this Table, respectively.

Table 1

General overview of the H_2O update in GEISA-2015

Isot. ID	**Wavenb. min (cm^{-1})**	**Wavenb. max (cm^{-1})**	**#lines**	**Moy. I (cm $molecule^{-1}$) at 296 K**	**Max. I (cm $molecule^{-1}$) at 296 K**	**Origin**
$H_2{}^{16}O$ 161	10.714930 5850.059600	5098.661059 7920.315400	12520 18757	$9.9741x10^{-30}$ $1.001x10^{-29}$	$2.651x10^{-18}$ $1.856x10^{-20}$	LISA, IAO LIPhy, IAO UMASS
$H_2{}^{17}O$ 171	0.451497 5850.241200 4174.108380	19945.257171 7905.615600 4299.793100	27547 3659 24	$4.857x10^{-35}$ $1.002x10^{-29}$ $6.46x10^{-28}$	$9.860x10^{-22}$ $6.939x10^{-24}$ $4.393x10^{-26}$	UCL LIPhy, IAO SRON, UMASS
$H_2{}^{18}O$ 181	893.551335 0.052583 4177.931920 5855.542000	1996.530386 19917.617846 4298.236000 7919.033200	974 39918 47 6641	$9.9741x10^{-30}$ $8.47x10^{-36}$ $2.93x10^{-26}$ $1.001x10^{-29}$	$2.651x10^{-18}$ $5.270x10^{-21}$ $2.440x10^{-25}$ $3.647x10^{-23}$	LISA UCL SRON LIPhy, IAO UMASS
$D_2{}^{16}O$ (new) 262	6378.9189 5.060500	6676.1465 7979.071900	225 5746	$7.31x10^{-33}$ $1.76x10^{-28}$	$2.640x10^{-31}$ $1.75x10^{-26}$	UCC, KIT IAO UMASS
$D_2{}^{18}O$ (new) 282	6328.068400	6637.658200	162	$9.41x10^{-35}$	$5.41x10^{-34}$	UCC, KIT UMASS

Below are some illustrations (non exhaustive display) of the GEISA-2015 H_2O update:

- A graphical overview of the GEISA-2015 line intensities for $H_2{}^{16}O$ is shown on Fig.1. The new intensity values cover the spectral regions: 10-5098 cm^{-1} **[2]**, 5850-7920 cm^{-1} **[3]**, and 7924-

9392 cm^{-1} **[7]**. Above 9500 cm^{-1} and, partly, between 1200 and 8000 cm^{-1}, the line intensities from GEISA-2011 were retained, these include data from Refs. **[8,9]**.

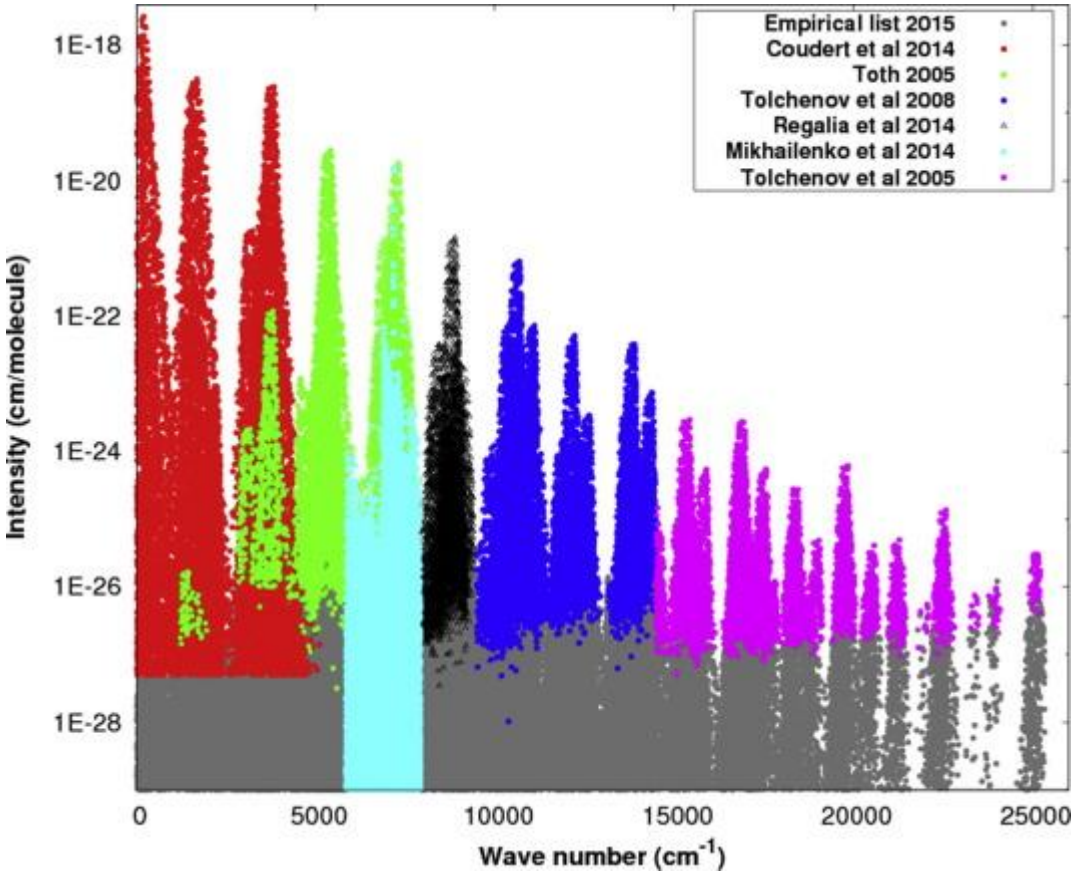

Fig. 1 Log scale graphical display of transition intensities (cm $molecule^{-1}$ at 296 K) included in GEISA-2015 for $H_2{}^{16}O$ **[1], [2], [3], [4], [5], [6], [9]**

- An illustration of the new line list (more than 29000 vibration-rotation transitions) on $H_2{}^{16}O$, $H_2{}^{17}O$, $H_2{}^{18}O$, in the 5850 - 7920 cm^{-1} spectral region (Mikhaïlenko et al. **[3])** is given, in Fig. 2, by the base 10 logarithm graphical display of intensities (cm $molecule^{-1}$) (Y-Axis) in the spectral range 5850-7920 cm^{-1} (X-abscissa).

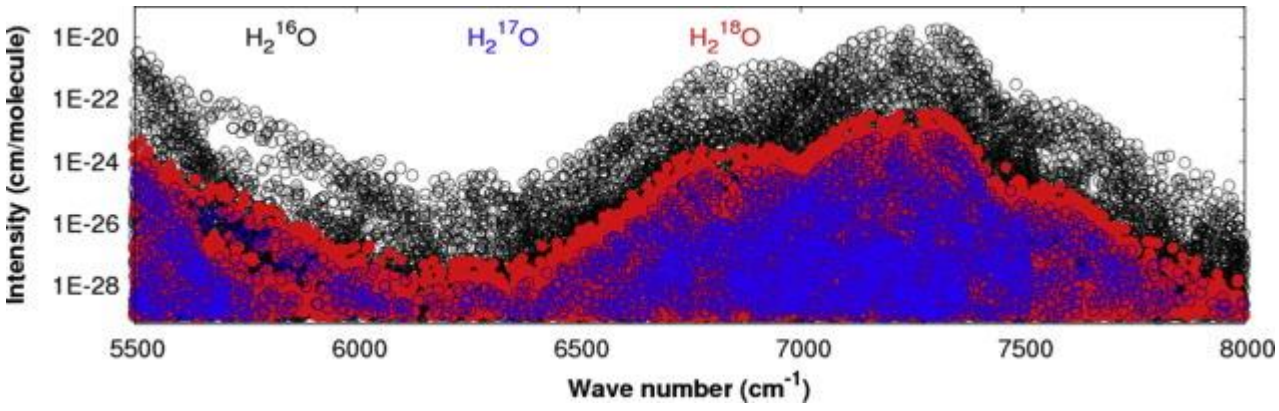

Fig. 2. Overview of line intensities (at 296 K, in logarithmic scale) in the GEISA-2015 line parameter database for water isotopologues, $H_2{}^{16}O$, $H_2{}^{17}O$, $H_2{}^{18}O$, between 5850 and 7920 cm^{-1}. The contribution of the different isotopologues is highlighted: $H_2{}^{16}O$ -black, $H_2{}^{17}O$ -blue, $H_2{}^{18}O$ -red).

Line shape parameters: the air-broadened half-widths, γ_{air}, its temperature dependence, n_{air}, the air-induced line shifts, δ_{air}, and the self-broadened half-widths, γ_{self}, are added to the GEISA-2015 database from a number of sources.

For the three most abundant isotopologues of water, $H_2{}^{16}O$, $H_2{}^{18}O$, and $H_2{}^{17}O$, the air-broadened half-widths, line shifts and self-broadened half-widths were added using a sophisticated scheme explained by Gordon et al. **[10]**. The temperature dependence of the half-width is taken from measured values, if no data exist the data are obtained from a polynomial in J" that was developed by Gamache **[11]** using the data of Birk and Wagner **[12]** smoothened and extrapolated to J"=50. Note, when there are no data available for $H_2{}^{18}O$ or $H_2{}^{17}O$, the corresponding data for $H_2{}^{16}O$ are used (if they exist).

For the air-D_2O collision system, measured half-widths and line shifts are available **[13-16]** for a small number of transitions in the ν_2, $2\nu_2$- ν_2, and ν_3 bands. From these data a set of air-broadened half-widths as a function of rotational quantum numbers was made and these data were added to the database neglecting vibrational dependence. To augment the measurement database, the half-width data were taken and the average half-width as a function of J" determined. There are no measured data on the temperature dependence of the half-width or on coefficient *n*. The HITRAN $H_2{}^{16}O$-air n values were used for $D_2{}^{16}O$-air with the error set to 50%.

For the D_2O-D_2O collision system, the half-width, its temperature dependence, and the line shift (rotation band only) data are from the MCRB calculations of Gamache et al. **[17]**. For transitions for which MCRB calculations are not available, the MCRB data were averaged as a function of J" and extrapolated to J"=50. The average values were then used for transitions for which there were no half-width data. The error in the averaged half-widths was set to 50%.

References

[1] O.V. Naumenko. Institute of Atmospheric Optics. Private communication. (2015).

[2] L.H. Coudert, M.-A. Martin-Drumell, O. Pirali, Analysis of the high-resolution water spectrum up to the Second Triad and to *J*=30, J. Mol. Spectrosc. 303 (2014) 36-41.

[3] S. Mikhailenko, D. Mondelain, S. Kassi, A. Campargue, An accurate and complete empirical line list for water vapor between 5850 and 7920 cm^{-1}, J. Quant. Spectrosc. Radiat. Trans. 140 (2014) 48-57.

[4] R.A. Toth, Measurements of positions, strengths and self-broadened widths of H_2O from 2900 to 8000 cm^{-1}: Line strength analysis of the 2nd triad bands, J. Quant. Spectrosc. Radiat. Trans. 94 (2005) 51-107.

[5] L. Régalia, C. Oudot, S. Mikhailenko, L. Wang, X. Thomas, A. Jenouvrier, P. Von der Heyden, Water vapor line parameters from 6450 to 9400 cm^{-1}, J. Quant. Spectrosc. Radiat. Trans. 136 (2014) 119-136.

[6] R. Tolchenov, J. Tennyson, Water line parameters from refitted spectra constrained by empirical upper state levels: Study of the 9500–14500 cm^{-1} region, J. Quant. Spectrosc. Radiat. Trans. 109 (2008) 559-568.

[7] J. Tennyson, P.F. Bernath, L.R. Brown, A. Campargue, A.G. Császár, L. Daumont, R.R. Gamache, J.T. Hodges, O.V. Naumenko, O.L. Polyansky, L.S. Rothman, A.C. Vandaele, N.F. Zobov, A.R. Al Derzi, C. Fábri, A.Z. Fazliev, T. Furtenbacher, I.E. Gordon, L. Lodi, I.I. Mizus, IUPAC critical evaluation of the rotational–vibrational spectra of water vapor. Part III: Energy levels and transition wavenumbers for $H_2{}^{16}O$, J. Quant. Spectrosc. Radiat. Trans. 117 (2013) 29-58.

[8] R.A. Toth, Line list of water vapor parameters from 500 to 8000 cm^{-1}, http://mark4sun.jpl.nasa.gov/h2o.html

[9] R.N. Tolchenov, O. Naumenko, N.F. Zobov, S.V. Shirin, O. L. Polyansky, J. Tennyson, M. Carleer, P.-F. Coheur, S. Fally, A. Jenouyrier, A.C. Vandaele, Water vapour line assignments in the 9250 – 26 000 cm^{-1} frequency range, J. Mol. Spectrosc. 233 (2005) 68-76.

[10] I.E. Gordon, L.S. Rothman, R.R. Gamache, D. Jacquemart, C. Boone, P.F. Bernath, M.W. Shephard, J.S. Delamere, S.A. Clough, Current updates of the water-vapor line list in *HITRAN*: A new "Diet" for air-broadened half-widths, J. Quant. Spectrosc. Radiat. Trans. 108 (2007) 389-402. doi:10.1016/j.jqsrt.2007.06.009.

[11] R.R. Gamache. University of Massachusetts Lowell. Unpublished results. (2014).

[12] M. Birk, G. Wagner, Temperatue-dependent air broadening of water in the 1250 – 1750 cm^{-1} range, J. Quant. Spectrosc. Radiat. Trans. 113 (2012) 889-928. doi:10.1016/j.jqsrt.2011.12.013.

[13] C.P. Rinsland, M.A.H. Smith, V. Malathy Devi, D. Chris Benner, Measurements of Lorentz-broadening coefficients and pressure-induced line shift coefficients in the υ_2 band of $D_2{}^{16}O$, J. Mol. Spectrosc. 150 (1991) 173-183.

[14] V. Malathy Devi, C.P. Rinsland, D. Chris Benner, M.A.H. Smith, Tunable diode laser measurements of air and N_2 broadened half-widths in the υ_2 band of D_2O, Appl. Opt. 25 (1986) 336-338.

[15] C.P. Rinsland, M.A.H. Smith, V. Malathy Devi, D. Chris Benner, Measurements of Lorentz-broadening coefficients and pressure-induced line shift coefficients in the υ_1 band of $HD^{16}O$ and the υ_3 band of $D_2{}^{16}O$, J. Mol. Spectrosc. 156 (1992) 507-511.

[16] R.A. Toth, Air- and N_2-broadening parameters of HDO and D_2O, 709 to 1931 cm^{-1}, J. Mol. Spectrosc. 198 (1999) 358-370.

[17] R.R. Gamache, M. Farese, C.L. Renaud, A spectral line list for water isotopologues in the 1100-4100 cm^{-1} region for application to CO_2-rich planetary atmospheres, J. Mol. Spectrosc. (in press). doi:10.1016/j.jms.2015.09.001.

CO_2 (molecule 2)

The GEISA-2011 carbon dioxide line list is replaced by the current version of CDSD-296 databank **[1]** which forms the new GEISA-2015 CO_2 line list. The CDSD-296 databank contains calculated line parameters (positions, intensities, air- and self-broadened half-widths, coefficients of temperature dependence of air-broadened half-widths and air pressure-induced line shifts) for twelve stable isotopic species of CO_2 (See Table 1 below). This databank was generated for a reference temperature 296 K and an intensity cut-off of 10^{-30} cm $molecule^{-1}$. It contains 534,227 lines covering the 6-14,075 cm^{-1} spectral range. The isotopologue composition of the current version of CDSD-296, and consequently in GEISA-2015, is presented in Table 1. The isotopologue Identification Codes (ID), respectively in CDSD, HITRAN-2012 and GEISA-2015, are listed in columns 1 to 3; column 4 and 5 detail the chemical formula and the natural abundance corresponding to each isotopologue; the number of lines reported for each species is in column 6.

Compared to GEISA-2011, the current version GEISA-2015 includes the spectral line parameters for three additional isotopologues: $^{17}O^{12}C^{17}O$, $^{17}O^{13}C^{18}O$ and $^{17}O^{13}C^{17}O$. The line parameters for other minor isotopologues are considerably improved and the spectral ranges extended.

Very recently Polyansky et al. computed an *ab-initio* dipole moment surface which has been used for the prediction of CO_2 intensities below 8000 cm^{-1} with very high accuracy **[2]**. This has been combined with energy levels from CDSD-296 to give a new line list for CO_2 **[3]** which will be considered as part of a future update.

Table 1

CO_2 isotopologues in GEISA-2015 (from Tashkun et al. **[1]**)

CDSD ID	HITRAN-2012 ID	GEISA-2015 ID	Molecular species	Abundance	#lines
1	1	626	$^{12}C^{16}O_2$	0.9842	170846
2	2	636	$^{13}C^{16}O_2$	1.106×10^{-2}	70462
3	3	628	$^{16}O^{12}C^{18}O$	3.947×10^{-3}	115942
4	4	627	$^{16}O^{12}C^{17}O$	7.339×10^{-4}	72120
5	5	638	$^{16}O^{13}C^{18}O$	4.434×10^{-5}	40143
6	6	637	$^{16}O^{13}C^{17}O$	8.246×10^{-6}	23901
7	7	828	$^{18}O^{12}C^{18}O$	3.957×10^{-6}	10593
8	8	728	$^{17}O^{12}C^{18}O$	1.472×10^{-6}	15206
9	9	727 (New)	$^{17}O^{12}C^{17}O$	1.430×10^{-7}	6623
10	0	838	$^{18}O^{13}C^{18}O$	4.446×10^{-8}	3111
11	Abs	738 (New)	$^{17}O^{13}C^{18}O$	1.654×10^{-8}	3621
12	Abs	737 (New)	$^{13}C^{17}O_2$	1.55×10^{-9}	1659

The algorithm to add CO_2 line shape parameters to the GEISA-2015 line list rely on data from the measurement database **[4]** and on rely on recent CRB calculations of the line shape parameters for CO_2 broadened by N_2, O_2, air, and CO_2 **[5-7]**. A study of the vibrational dependence of the half-width and line shift, and the temperature dependence of these parameters was recently completed by Gamache and Lamouroux **[8]**. From this study they developed an algorithm based on a generalization of the method of Gamache and Hartmann **[9]** that can predict the line shape parameters for CO_2 in collision with N_2, O_2, air, and CO_2 **[10]**. Using the algorithm, the half-width, its temperature dependence, and the line shift for both air- and self-broadening of CO_2, and the corresponding errors in these parameters were added to the GEISA-2015 CO_2 transitions.

References

[1] S.A. Tashkun, V.I. Perevalov, R.R. Gamache, J. Lamouroux, CDSD-296, high resolution carbon dioxide spectroscopic databank: Version for atmospheric applications, J. Quant. Spectrosc. Radiat. Transfer 152 (2015) 45–73.

[2] O.L. Polyansky, K. Bielska, M. Ghysels, L. Lodi, N.F. Zobov, J.T. Hodges and J. Tennyson, High accuracy CO_2 line intensities determined from theory and experiment, Phys. Rev. Lett. 114 (2015) 243001.

[3] E. Zak, J. Tennyson, O.L. Polyansky, L. Lodi, S.A. Tashkun and V.I. Perevalov, A room temperature CO_2 line list with ab initio computed intensities, J. Quant. Spectrosc. Rad. Transfer 177 (2016) 31-42.

[4] R.R. Gamache, J. Lamouroux, V. Blot-Lafon, E. Lopes, An intercomparison of measured pressure-broadening, pressure shifting parameters of carbon dioxide and their temperature dependence, J. Quant. Spectrosc. Radiat. Transfer 135 **(**2014) 30-43.

[5] R.R. Gamache, J. Lamouroux, A.L. Laraia, J.-M. Hartmann, C. Boulet, Semiclassical calculations of half-widths and line shifts for transitions in the 30012←00001 and 30013←00001 bands of CO_2 I: Collisions with N_2, J. Quant. Spectrosc. Radiat. Transfer 113 (2012) 976-990.

[6] J. Lamouroux, R.R. Gamache, A.L. Laraia, J.-M. Hartmann, C. Boulet, Semiclassical calculations of half-widths and line shifts for transitions in the 30012←00001 and 30013←00001 bands of CO_2 II: collisions with O_2 and Air, J. Quant. Spectrosc. Radiat. Transfer 113 (2012) 991-1003.

[7] J. Lamouroux, R.R. Gamache, A.L. Laraia, J.-M. Hartmann, C. Boulet, Semiclassical calculations of half-widths and line shifts for transitions in the 30012←00001 and 30013←00001 bands of CO_2 III: self collisions, J. Quant. Spectrosc. Radiat. Transfer 113 (2012) 1536-1546.

[8] R.R. Gamache, J. Lamouroux, The vibrational dependence of half-widths of CO_2 transitions broadened by N_2, O_2, air, and CO_2, J. Quant. Spectrosc. Radiat. Transfer 117 **(**2012) 93-103.

[9] R.R. Gamache, J.-M. Hartmann, Collisional parameters of H_2O lines: effects of vibration, J. Quant. Spectrosc. Radiat. Transfer 83 **(**2004) 119-147.

[10] R.R Gamache, J. Lamouroux, Predicting accurate line shape parameters for CO2 transitions, J. Quant. Spectrosc. Radiat. Transfer 130 **(**2013) 158-171.

O_3 (molecule 3)

In GEISA-2015 the ozone line list is considerably extended and is now almost complete up to nearly 7000 cm^{-1}. The new line list was generated using results reported by Barbe et al.**[1]**.

Forty-six bands of the main ozone isotopologue, $^{16}O_3$, in the 3266-6997 cm^{-1} spectral region are newly included in the GEISA-2015 database, as summarized in Table 1. The twenty-four bands up to 5800 cm^{-1} were obtained from the analysis of FTS recorded in GSMA laboratory of Reims University **[1-6,11],** while the twenty two other bands were recorded by CW-CRDS in LIPhy laboratory of Grenoble University **[7-10]**. All these data are implemented in the S&MPO databank (Babikov et al. [**11]**)**,** jointly developed and maintained by the Institute of Atmospheric Optics (Tomsk) and Reims University.

Table 1

Ozone bands newly included or updated in GEISA-2015 line parameter database. Upper and lower state vibrational band identifiers (v_i (i=1,2,3)) are given in column 1, with associated number of archived lines, spectral region in cm^{-1}, total intensity in cm $molecule^{-1}$ at 296 K, and source references, in columns 2 to 5, respectively.

Band	**# lines**	**Spectral region (cm^{-1})**	**S_V (cm molecule $^{-1}$ at 296 K)**	**Refs.**
022 – 000	2616[a]	3266.51 – 3488.18	1.111×10^{-22}	**[1]**
121 – 000	2210[a]	3373.90 – 3487.30	6.329×10^{-22}	**[1]**
220 – 000	684[a]	3488.15 – 3627.87	2.500×10^{-23}	**[1]**
311 – 100	729	3739.97 – 3826.22	2.398×10^{-23}	**[2]**
005 – 100	508	3742.91 – 3726.13	1.660×10^{-23}	**[2]**
104 – 100	51	3752.69 – 3863.55	8.192×10^{-25}	**[2]**
005 – 001	278	3807.31 – 3917.54	9.849×10^{-24}	**[2]**
311 – 001	436	3810.30 – 3946.73	9.846×10^{-24}	**[2]**
104 – 001	950	3820.17 – 3894.94	2.218×10^{-22}	**[2]**
123 – 010	783	4531.73 – 4599.39	6.534×10^{-23}	**[3]**
330 – 010	47	4554.65 – 4601.97	1.830×10^{-24}	**[3]**
104 – 000	1093	4802.98 – 4978.61	7.789×10^{-23}	**[2]**
005 – 000	1514	4806.33 – 4938.21	5.300×10^{-22}	**[2]**
311 – 000	1053	4827.65 – 4928.49	3.450×10^{-22}	**[2]**
203 – 000	1086	4997.30 – 5085.47	1.263×10^{-22}	**[4]**
132 – 000	27	5028.06 – 5085.33	1.396×10^{-24}	**[4]**
123 – 000	784	5216.76 – 5300.21	5.902×10^{-23}	**[3]**
401 – 000	896	5244.80 – 5319.26	8.153×10^{-23}	**[3]**
330 – 000	43	5252.48 – 4302.26	1.514×10^{-24}	**[3]**
024 – 000	2	5271.73 – 5316.28	6.791×10^{-26}	**[3]**
015 – 000	622	5625.97 – 5704.62	3.465×10^{-23}	**[3]**
420 – 000	10	5663.20 – 5706.33	3.065×10^{-25}	**[3]**
105_1 – 000 [c]	730	5708.95 – 5790.90	4.943×10^{-23}	**[6]**
312 – 000	14	5753.33 – 5786.12	4.336×10^{-25}	**[6]**
421 – 010	303	5815.58 – 5873.74	3.570×10^{-25}	**[9]**
133 – 000	702	5852.44 – 5931.22	4.718×10^{-24}	**[9]**
411 – 000	444	5895.17 – 5956.76	1.379×10^{-24}	**[9]**
233_1 – 000 [c]	528	5941.73 – 6021.44	7.950×10^{-25}	**10]**
034 – 000	264	5956.88 – 6078.00	8.529×10^{-25}	**[7]**
105_2 – 000 [c]	678	5983.44 – 6071.43	2.097×10^{-24}	**[7]**
124_1 – 000 [c]	999	6019.98 – 6201.30	2.934×10^{-24}	**[7]**
223_1 – 000 [c]	954	6031.75 – 6130.78	1.179×10^{-23}	**[7]**
510 – 000	39	6067.96 – 6136.40	$1.275 \text{ X } 10^{-25}$	**[7]**
331 – 000	168	6163.49 – 6207.75	1.371×10^{-25}	**[7]**
025 – 000	1003	6225.12 – 6311.46	7.702×10^{-24}	**[8]**
124_2 – 000 [c]	78	6246.40 – 6363.42	3.445×10^{-25}	**[8]**
430 – 000	111	6284.63 – 6395.38	3.115×10^{-25}	**[8]**
501 – 000	749	6301.80 – 6365.48	6.370×10^{-24}	**[8]**
223_2 – 000 [c]	777	6318.03 – 6393.74	6.790×10^{-24}	**[8]**
421 – 000	409	6503.67 – 6574.40	8.695×10^{-25}	**[9]**
205_1 – 000 [c]	570	6525.82 – 6593.61	1.966×10^{-24}	**[9]**
242 – 000	457	6665.49 – 6822.32	2.914×10^{-25}	**[10]**
233_1 – 000 [c]	754	6641.08 – 6722.18	1.583×10^{-24}	**[10]**

Band	# lines	Spectral region (cm^{-1})	S_V (cm molecule $^{-1}$ at 296 K)	Refs.
520 – 000	33	6677.10 – 6771.82	2.158×10^{-26}	**10]**
511 – 000	317[b]	6945.09 – 6989.76	2.423×10^{-25}	**[9]**
233_2 – 000 [c]	417	6950.18 – 6996.68	4.506×10^{-25}	**[9]**

Notes: [a,b)] The number of transitions is not the same as that given in the S&MPO databank [**11]** due to use of a cut-off of respectively 3×10^{-27} instead of 2×10^{-26} and 1×10^{-28} instead of 2×10^{-28} (in cm molecule^{-1}).
[c)] For these bands the additional ranking number is given to distinguish the upper states which could have the same principal normal mode contributions as discussed in **[12]**; S_V is the integrated band intensity computed as a sum of vibration-rotation line intensities with the I_{min} and J_{max} cut-off specified for each band in original publications cited in the last column.

A graphical intensity overview of the new data is shown on Fig. 1.

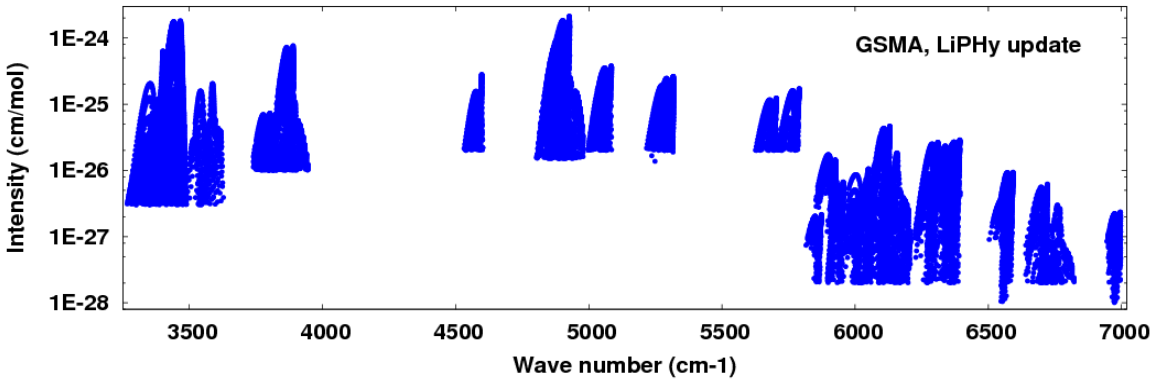

Fig. 1. Overview of line intensities of the supplementary ozone data included in GEISA-2015 in the 3266-6997 cm^{-1} spectral region. The intensity cut-off is much lower above 5800 cm^{-1} because the laser CRDS measurements in this range were more sensitive resulting in the detection and assignments of much weaker lines **[8-10].**

All these data are implemented in the S&MPO databank (Babikov et al. **11]),** jointly developed and maintained by the Institute of Atmospheric Optics (Tomsk) and Reims University.

Fig. 2 exhibits the difference of ozone absorption between 3397.3 and 3404.7 cm^{-1} using GEISA-2011 (upper panel A) and GEISA-2015 (lower panel B). On each panel, the upper part displays the experimental (in blue) and simulated (in olive) transmission spectra in %. The lower part displays the difference (in %) between the experimental ("OBS") and simulated transmission based on GEISA-2011 (panel A) and GEISA-2015 (panel B). The sum of the squares of differences between observed and simulated spectra ($Diff = \sum_{i=1}^{n} (T_i^{Obs} - T_i^{Simul})^2$, n – number of spectrum points,

T- transmission) are 0.560 and 0.064 for GEISA-2011 and GEISA-2015 respectively. The new line list (GEISA-2015) was generated using results reported by Barbe et al.**[1]**.

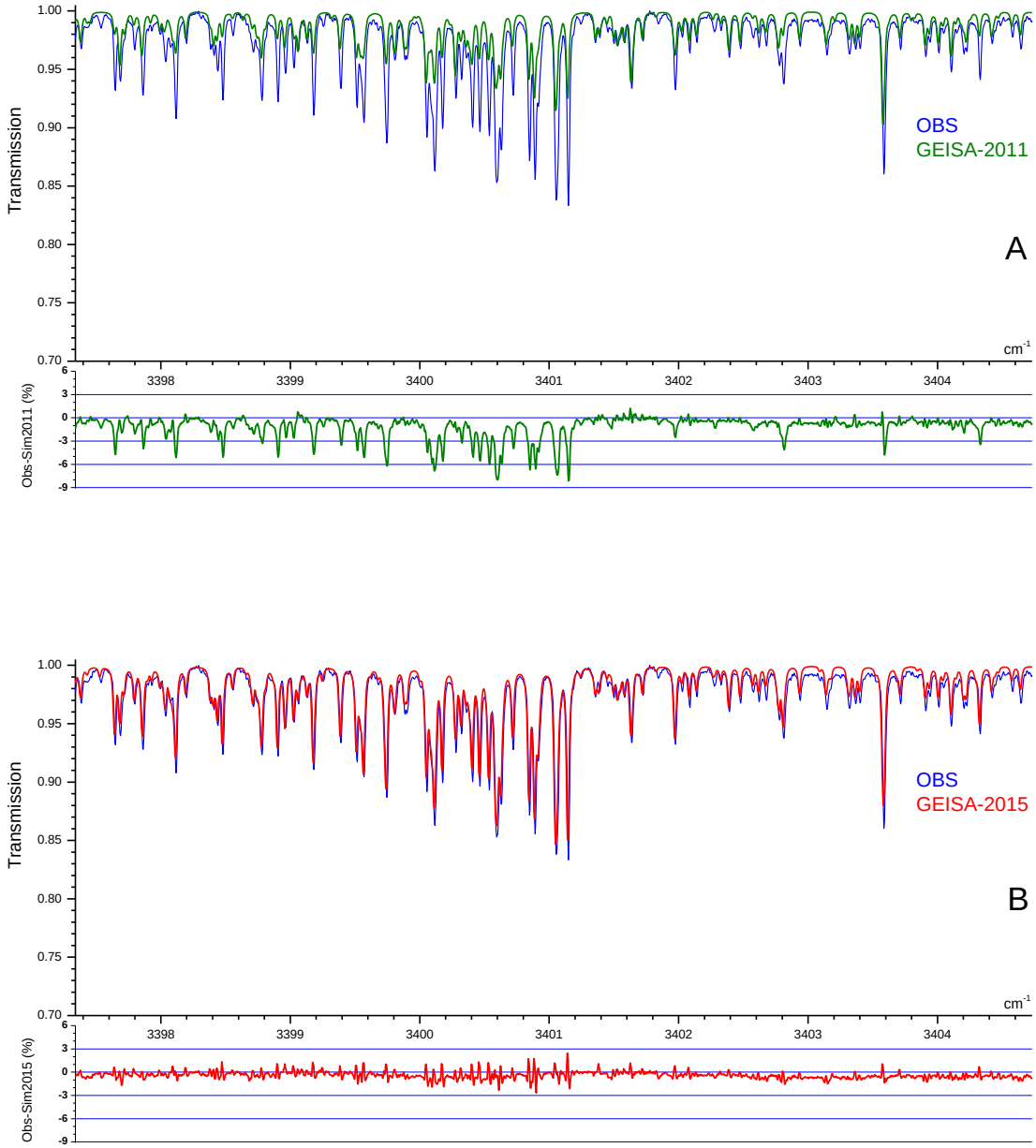

Fig.2. Differences between ozone absorption simulations using GEISA-2011 (upper panel A) and GEISA-2015 (lower panel B) for the $\nu_1+2\nu_2+\nu_3$ and $2\nu_2+2\nu_3$ bands near 3400 cm^{-1}.

References

[1] A. Barbe, M.-R. De Backer, E. Starikova, S.A. Tashkun, X. Thomas, Vl.G. Tyuterev, FTS high resolution spectra of $^{16}O_3$ in 3500 and 5500 cm^{-1} regions. First example of new theoretical modelling for a polyad of strongly coupled states, J. Quant. Spectrosc. Radiat. Transfer 113 (2012) 829-839.

[2] A. Barbe. Université de Reims Champagne-Ardenne. Private communication. (2011).

[3] A. Barbe, J.J. Plateaux, S.N. Mikhailenko, Vl.G. Tyuterev, Infrared spectrum of ozone in the 4600 and 5300 cm^{-1} regions: High order accidental resonances through the analysis of the $\nu_1+2\nu_2+3\nu_3-\nu_2$, $\nu_1+2\nu_2+3\nu_3$, and $4\nu_1+\nu_3$ bands, J. Molec. Spectrosc. 185 (1997) 408-416.

[4] A. Barbe, J.J. Plateaux, Vl.G. Tyuterev, S.N. Mikhailenko, Analysis of high resolution measurements of the $2\nu_1+3\nu_3$ band of ozone: Coriolis interaction with the $\nu_1+3\nu_2+2\nu_3$ band, J. Quant. Spectrosc. Radiat. Transfer 59 (1998) 185-194.

[5] A. Barbe, A. Chichery, The $2\nu_1+\nu_2+3\nu_3$ band of $^{16}O_3$. Line positions and intensities, J. Molec.Spectrosc. 192 (1998) 102-110.

[6] A. Barbe, A. Chichery, Vl.G. Tyuterev, J.J. Plateaux, Analysis of high resolution measurements of the $\nu_1+5\nu_3$ band of ozone: Coriolis interactions with the $6\nu_3$ and $3\nu_1+\nu_2+2\nu_3$ bands, Molec.Phys. 94 (1998) 751-757.

[7] A. Barbe, M.-R. De Backer, Vl.G. Tyuterev, A. Campargue, D. Romanini, S. Kassi, CW-cavity ring down spectroscopy of ozone molecule in the 5980 – 6220 cm^{-1} region, J. Molec.Spectrosc. 242 (2007) 156-175.

[8] A. Barbe, M.-R. De Backer, Vl.G. Tyuterev, S. Kassi, A. Campargue, CW-cavity ring down spectroscopy of ozone molecule in the 6220 – 6400 cm^{-1} region, J. Molec.Spectrosc. 246 (2007) 22-38.

[9] A. Campargue, M.-R. De Backer-Barilly, A. Barbe, Vl.G. Tyuterev, S. Kassi, The near infrared spectrum of ozone by CW-cavity ring down spectroscopy between 5850 and 7000 cm^{-1}: New observations and exhaustive review, Phys. Chem. Chem. Phys. 10 (2008) 2925-2946.

[10] A. Campargue, S. Kassi, D. Romanini, A. Barbe, M.-R. De Backer, Vl.G. Tyuterev, CW-cavity ring down spectroscopy of ozone molecule in the 6625-6830 cm^{-1} region, J. Molec.Spectrosc. 240 (2006) 1-13.

[11] Y.L. Babikov, S.N. Mikhailenko, A. Barbe, Vl.G. Tyuterev, S&MPO – an information system for ozone spectroscopy on the WEB, J. Quant. Spectrosc. Radiat. Transfer 145 (2014) 169-196.

[12] A. Barbe, S. Mikhailenko, E. Starikova, M.-R. De Backer, Vl.G. Tyuterev, D. Mondelain, S. Kassi, A. Campargue, C. Janssen, S. Tashkun, R. Kochanov, R. Gamache. Ozone spectroscopy in the electronic ground state: High resolution spectra analyses and update of line parameters since 2003. J. Quant. Spectrosc. Radiat.Transfer 130 (2013) 172-190.

CH_4 (molecule 6)

Part of the GEISA-2015 methane update is based on the latest global fits of line-by-line assignments (for both line positions and line intensities). The global analysis up to the Tetradecad region **[1]** was used for $^{12}CH_4$, while a global fit up to the Octad region **[2]** was used for $^{13}CH_4$. The line list was generated by computing semi-empirical upper state energy levels. These levels are calculated from averages over several transitions sharing the same upper state; all line positions are then recomputed using these upper states. This method is the same as the one used for the HITRAN-2012 methane update described in Ref. **[3]**. In the case of $^{12}CH_4$, the calculated lines of Octad–Dyad resulting from these global fits are discarded in the present GEISA update, while Octad–Pentad lines are included with an intensity cut-off limited to 10^{-26} cm^{-1}/molecule cm^{-2}. Moreover, after a careful validation process based on a method described in Armante et al. **[4]**, it appeared that the new spectroscopic parameters of the Octad–GS lines for $^{12}CH_4$ and $^{13}CH_4$, and the

Dyad–GS lines for $^{13}CH_4$, were less precise than the previous ones in GEISA-2011**;** these have, consequently, been retained in GEISA-2015.

The present calculated data were recently used to estimate the spectroscopic uncertainties for methane retrievals associated with the set-up and instrumentation of the future Earth-observing satellite Sentinel-5 **[5].**

The near infrared line list for methane above 5850 cm^{-1} has been considerably updated on the basis of new measurements. In the recent years, considerable progress has been achieved using new measurements with increased sensitivity and extended spectral coverage. The major changes are illustrated in the overview comparison of the GEISA-2011 and GEISA-2015 line lists presented in Fig.1.

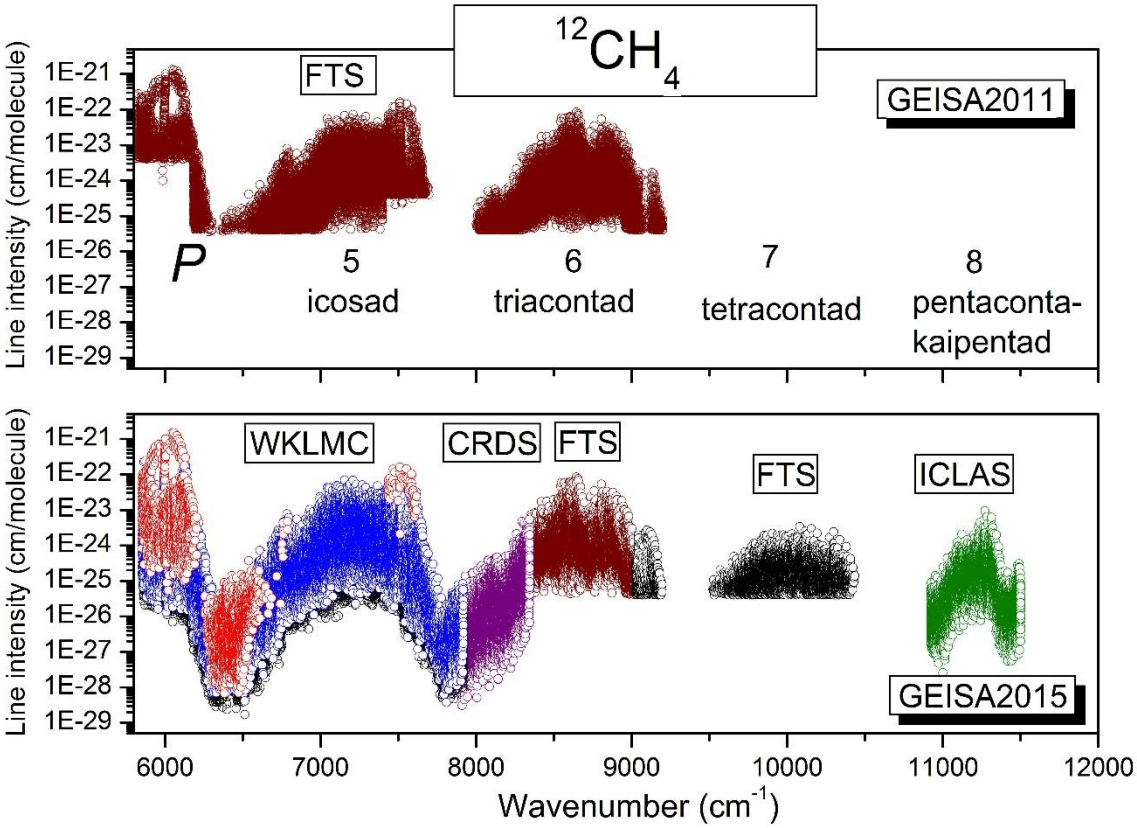

Fig. 1. Line intensity overview comparison of the GEISA list of $^{12}CH_4$ in the 2011 and 2015 editions of GEISA above 5850 cm^{-1}. In this region, line parameters all are of empirical origin: the WKLMC list up to 7920 cm^{-1} **[7]**, CRDS between 7920 and 8345 cm^{-1} **[8]**, FTS by Brown in the 8345-9028 cm^{-1} interval **[6]** and by Béguier et al. in the 9028-10923 cm^{-1} interval **[9]**, and ICLAS between 11000 and 11500 cm^{-1} **[10]**. The different polyad and corresponding numbers, *P*, are indicated. (The polyad number *P* is equal to $2(V_1+V_3)+V_2+V_4$, where V_i are the normal mode vibrational quantum numbers). The WKLMC lines with full rovibrational assignments or E_{emp} values have been highlighted with red and blue symbols, respectively.

References

[1] A. Nikitin, V. Boudon, Ch. Wenger, S. Albert, L. R. Brown, S. Bauerecker, M. Quack, High Resolution Spectroscopy and First Global Analysis of the Tetradecad Region of Methane $^{12}CH_4$. Phys. Chem. Chem. Phys, 15 (2013) 10071–10093.

[2] H.-M. Niederer, X.-G. Wang, T. Carrington Jr., S. Albert, S. Bauerecker, V. Boudon, Analysis of the rovibrational spectrum of methane $^{13}CH_4$ in the infrared, J. Molec. Spectrosc. 291 (2013) 33–47.

[3] L. R. Brown, K. Sung, D. C. Benner, V. M. Devi, V. Boudon, T. Gabard, Ch. Wenger, A. Campargue, O. Leshchishina, S. Kassi, D. Mondelain, L. Wang, L. Daumont, L. Régalia, M. Rey, X. Thomas, Vl. G. Tyuterev, O. M. Lyulin, A. V. Nikitin, H. M. Niederer, S. Albert, S. Bauerecker, M. Quack, J. J. O'Brien, I. E. Gordon, L. S. Rothman, H. Sassada, A. Coustenis, M. A. H. Smith, T. Carrington Jr., X. G. Wang, A. W. Manz, P. T. Spickler, Methane Line Parameters in the HITRAN Database, J. Quant. Spectrosc. Radiat. Transf. 130 (2013) 201–219.

[4] R. Armante, N.A. Scott, C. Crevoisier, V. Capelle, L. Crépeau, N. Jacquinet, A. Chédin, Evaluation of spectroscopic databases through radiative transfer simulations compared to observations. Application to the validation of GEISA-2015 with IASI and TCCON, J. Molec. Spectrosc. 327 (2016) 180–192, http://dx.doi.org/10.1016/j.jms.2016.04.004

[5] R. Checa-Garcia, J. Landgraf, A. Galli, F. Hase, V. A. Velazco, H. Tran. V. Boudon, F. Alkemade, A. Butz, Mapping spectroscopic uncertainties into prospective methane retrieval errors from Sentinel-5 and its precursor, 8 (2015) 3617–3629.

[6] L. Brown, Empirical line parameters of methane from 1.1 to 2.1 μm, J. Quant. Spectrosc. Radiat. Transf. 96 (2005) 251–270.

[7] A. Campargue, O. Leshchishina, L. Wang, D. Mondelain, S. Kassi, The WKLMC empirical line lists (5852–7919cm^{-1}) for methane between 80K and 296K: "final" lists in HITRAN format for atmospheric and planetary applications, J. Molec. Spectrosc. 291 (2013) 16–22.

[8] S. Béguier, S. Kassi, A. Campargue, An empirical line list for methane in the 1.25 μm transparency window, J. Molec. Spectrosc. 308–309 (2015) 1–5.

[9] S. Béguier, A. W. Liu, A. Campargue, An empirical line list for methane near 1 μm (9028-10435 cm^{-1}), J. Quant. Spectrosc. Radiat. Transf. 166 (2015) 6–12.

[10] D. Chris Benner, V. Malathy Devi, J.J. O'Brien, S. Shaji, P.T. Spickler, C.P. Houck, J.A. Coakley, J. Dolph, K. Rankin, Empirical line parameters of CH_4 from 10923 to 11502 cm^{-1}, in preparation. Private communication 2015.

O_2 (molecule 7)

The GEISA-2015 update has started from the O_2 line list as given in HITRAN-2012, which represents a substantial extension to previous versions of GEISA and HITRAN, with updates largely based on Gordon et al. **[1,2]**, Leshchishina et al. **[3,4]** and Long et al. **[5-7]**. The line positions and lower states energies were updated with the results from an updated isotopically invariant Dunham fit published by Yu et al. in 2014 **[8]**. The other line parameters, such as line intensities and broadening, remain unchanged, and finally the number of lines also stays the same. The new microwave work **[9]** measured 324 rotational transitions in the $a^1\Delta_g$ v = 0 and 1 states of the six O_2 isotopologues with experimental accuracy of 50-200 kHz, which helped determine two more hyperfine parameters, the electric quadrupole interaction *eQq* and the nuclear spin-rotation

interaction C_I. The new infrared work **[10]** reported 1644 transition frequencies in the $b^1\Sigma_g^+ - X^3\Sigma_g^-$ system of six O_2 isotopologues and the experimental accuracy ranged from 0.0004 to 0.006 cm^{-1}.

When compared to HITRAN-2012, line positions differences up to 0.015 cm^{-1} were found for the $^{16}O^{16}O$ *a* – *X* system, up to 0.05 cm-1 for $^{16}O^{16}O$ *b* – *X*, up to 0.05 cm^{-1} for $^{16}O^{17}O$ *a* – *X*, up to 0.025 cm^{-1} for $^{16}O^{17}O$ *b* – *X*, up to 0.003 cm^{-1} for $^{16}O^{18}O$ *a* – *X* system, and up to 0.09 cm^{-1} for $^{16}O^{18}O$ *b* – *X*. Fig. 1 presents a comparison of the $^{16}O^{17}O$ *a* – *X*(v', v") = (0,0) band position with experiment, which indicates a systematic error in the line positions of this band in HITRAN-2012 which has been corrected in GEISA-2015.

It was found that in HITRAN-2012, the quantum numbers for the Δ*NΔJ*= *PO* branch of the $^{16}O^{16}O$ *a* – *X*(v', v") = (0,0) band were incorrectly labeled, i.e., the 7875.6 cm^{-1} transition with a lower state energy of 16.4 cm^{-1} was labeled as *P*1*O*2. A *P*1*O*2 line has *N''*=1, *J''*=2, *N'*=0 and *J'*=0, but the rotational level of *N'*=0 and *J'*=0 does not exist in the $a^1\Delta_g$ state. The correct assignment for this line is *P*3*O*4. Other lines in the same *PO* branch were also incorrectly labeled with the same shift of two in quantum numbers. This error is corrected in the updated GEISA-2015 line list.

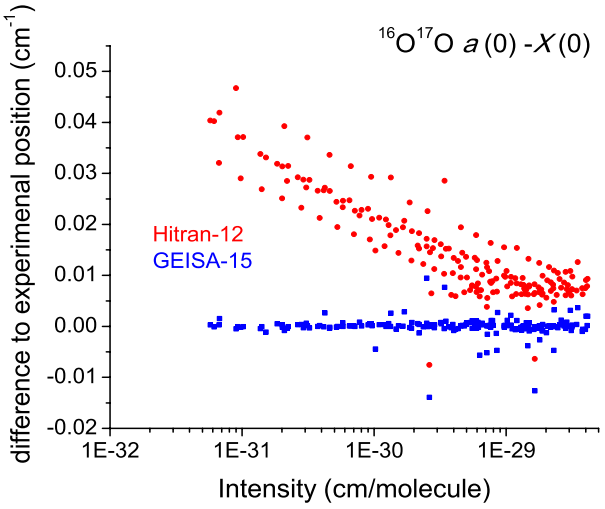

Fig.1. Comparisons of the $^{16}O^{17}O$ $a^1\Delta_g - X^3\Sigma_g^-$ (v', v") = (0,0) band positions in HITRAN-2012 (red) and GEISA-2015 (blue) as a function of the intensity.

References

[1] I. E. Gordon, S. Kassi, A. Campargue, G. C. Toon, First identification of the electric quadrupole transitions of oxygen in solar and laboratory spectra, J. Quant. Spectrosc. Radiat. Transfer 111 (2010), 1174 – 1183.

[2] I. E. Gordon, L. S. Rothman, G. C. Toon, Revision of spectral parameters for the B- and □ □-bands of oxygen and their validation against atmospheric spectra, J. Quant. Spectrosc. Radiat. Transfer 112 (2011), 2310 – 2322.

[3] O. Leshchishina, S. Kassi, I. E. Gordon, L. S. Rothman, L. Wang, A. Campargue, High sensitivity CRDS of the $a^1\Delta_g - X^3\Sigma_g^-$ band of oxygen near 1.27μm: Extended observations, quadrupole transitions, hot bands and minor isotopologues, J. Quant. Spectrosc. Radiat. Transfer 111 (2010), 2236 – 2245.

[4] O. Leshchishina, S. Kassi, I. E. Gordon, S. Yu, A. Campargue, The $a^1\Delta_g - X^3\Sigma_g^-$ band of $^{16}O^{17}O$, $^{17}O^{18}O$ and $^{17}O_2$ by high sensitivity CRDS near 1.27□m, J. Quant. Spectrosc. Radiat. Transfer 112 (2011), 1257 – 1265.

[5] D. A. Long, D. K. Havey, M. Okumura, H. M. Pickett, C. E. Miller and J. T. Hodges, Laboratory measurements and theoretical calculations of O_2 A-band electric quadrupole transitions, Phys. Rev. A 80 (2009), 042513.

[6] D. A. Long, D. K. Havey, M. Okumura, C. E. Miller and J. T. Hodges, O_2 A-band line parameters to support atmospheric remote sensing, J. Quant. Spectrosc. Radiat. Transfer 111 (2010), 2021 – 2036.

[7] D. A. Long, D. K. Havey, S. Yu, M. Okumura, C. E. Miller, J. T. Hodges, O_2 A-band line parameters to support atmospheric remote sensing. Part II: The rare isotopologues, J. Quant. Spectrosc. Radiat. Transfer 112 (2011), 2527 – 2541.

[8] S. Yu, B. Drouin, and C. Miller, High resolution spectral analysis of oxygen IV. Energy levels, partition sums, band constants, RKR potentials, Franck-Condon factors involving the $X^3\Sigma_g^-$, $a^1\Delta_g$, and $b^1\Sigma_g^+$ states, J. Chem. Phys. 141 (2014), 174302.

[9] B. Drouin, H. Gupta, S. Yu, C. Miller, and H. Muller, High resolution spectral analysis of oxygen II. rotational spectra of $a^1\Delta_g$ O_2 isotopologues, J. Chem. Phys. 137 (2012), 024305.

[10] B. Drouin, S. Yu, B. Elliott, T. Crawford, and C. Miller, High resolution spectral analysis of oxygen III. Laboratory investigation of the airglow bands, J. Chem. Phys. 139 (2013), 144301.

SO_2 (molecule 9)

The basis for GEISA-2015 update relies on an entry of the CDMS catalog for the ν_2 band which is based on extensive rotational transitions in its $v_2 = 0$ and 1 states **[1]** along with previous IR data . A total revision of the $v_2 = 0$ and $v_2 = 1$ rotational transitions has been made, using data from the CDMS catalog. The spectroscopic data of two (as identified in the CDMS catalog) data files, i.e.: (i) W064502 (transition 000-000), 14754 entries; version 2; (ii) W064503 (transition 010-010), 9808 entries; version 2, have been implemented in GEISA-2015 and used to totally replace previous data, after unit conversion and line shape default value addition, i.e.:

- HWHM (γ_{air}) default value=0.1100 cm^{-1} atm^{-1}
- HWHM self (γ_{self}) default value=0.400 cm^{-1} atm^{-1}

A constant default value of 0.75 has been adopted for the temperature dependence coefficient *n* of the air-broadening half width. The air pressure shift is set at the value 0.0 $cm^{-1}atm^{-1}$ at 296 K.

Besides new or updated transition frequencies from Ref. **[1]**, important data sources in this new study on rotational transitions in the ground and v_2=1 states are those of Belov et al. **[2]** and Müller et al. **[3]** for the ground vibrational state as well as those of Mehrotra et al. **[178,179]**, Helminger and DeLucia **[6]**, and Alekseev et al. **[7]** v_2=0 and 1.

The predictions should be accurate enough for observational purposes at temperatures up to about 300 K because uncertainties become noticeable only for very weak transitions. The data may have to be viewed with some caution at temperatures much higher than 300 K.

References

[1] H.S.P. Müller, S. Brünken, Accurate rotational spectroscopy of sulfur dioxide, SO_2, in its ground vibrational and first excited bending states, $v_2 = 0$, 1, up to 2 THz, J. Mol. Spectrosc. 232 (2005) 213–222.

[2] S.P. Belov, M.Yu. Tretyakov, I.N. Kozin, E. Klisch, G. Winnewisser, W.J. Lafferty, J.-M. Flaud, High Frequency Transitions in the Rotational Spectrum of SO_2, J. Mol. Spectrosc. 191 (1998) 17–27.

[3] H.S.P. Müller, J. Farhoomand, E.A. Cohen, B. Brupbacher-Gatehouse, M. Schäfer, A. Bauder, G. Winnewisser, The Rotational Spectrum of SO_2 and the Determination of the Hyperfine Constants and Nuclear Magnetic Shielding Tensors of $^{33}SO_2$ and $SO^{17}O$, J. Mol. Spectrosc. 201 (2000) 1–8.

[4] S.C. Mehrotra, G. Bestmann, H. Dreizler, H. Mäder, Contribution to the investigation of T_2-relaxation: rotational transitions of OCS and SO_2, Z. Naturforsch. 39a (1984) 633–636.

[5] S.C. Mehrotra, H. Dreizler, H. Mäder, *J*-Dependence of T_2-parameters for rotational transitions of SO_2 and CH_3OH in *K*-band, Z. Naturforsch. 40a (1985) 683–685.

[6] P.A. Helminger, F. DeLucia, The submillimeter wave spectrum of $^{32}S^{16}O_2$, $^{32}S^{16}O_2$ (v_2), and $^{34}S^{16}O_2$, J. Mol. Spectrosc. 111 (1985) 66–72.

[7] E.A. Alekseev, S.F. Dyubko, V.V. Ilyushin, S.V. Podnos, The High-Precision Millimeter-Wave Spectrum of $^{32}SO_2$, $^{32}SO_2$ (v_2), and $^{34}SO_2$. J. Mol. Spectrosc. 176 (1996) 316–320.

NH_3 (molecule 11)

Down et al. **[1]** performed a thorough re-analysis of the available experimental data for $^{14}NH_3$. They generated a set of empirical energy levels and used the BYTe line list **[2]** to both make new assignments and to correct old ones. At the same time Down et al. **[1]** proposed a new and consistent set of quantum numbers which they applied to their data. Finally they used their empirical energy levels and BYTe intensities to generate new line lists for the $\nu_2 + \nu_4 - \nu_4$, $\nu_4 - \nu_2$, $\nu_4 - \nu_4$, and $2\nu_2 - 2\nu_2$ hot bands. These data have been used to update the NH_3 GEISA-2015 line list. This represents a total of 40,224 entries.

In the previous editions of GEISA, the NH_3 archive ended near 5294 cm^{-1}. In 2015, it was extended to 7000 cm^{-1} using 5100 entries of the empirical line list from Sung et al. **[3]**. However, no compilations were created for missing ammonia bands between 5300 and 6300 cm^{-1}, and no improved analyses were made for the existing $^{15}NH_3$ entries.

The new consistent set of quantum numbers proposed by Down et al**. [1]** has been applied to the data of Sung et al. **[3]**, as well**.**

References

[1] M.J. Down, C. Hill, S.N. Yurchenko, J. Tennyson, L.R. Brown, I. Kleiner, Re-analysis of ammonia spectra: Updating the HITRAN $^{14}NH_3$ database, J. Quant. Spectrosc. Radiat. Transfer 130 (2013) 260-272.

[2] N. Yurchenko, R.J. Barber, J. Tennyson, A variationally computed hot line list for NH_3, Mon. Not. R. astron. Soc. 413 (2011) 1828-1834.

[3] K. Sung, L. R. Brown, X. Huang, D. W. Schwenke, T. J. Lee, S. L. Coy, K. K. Lehmann, Extended line positions, intensities, empirical lower state energies and quantum assignments of NH_3 from 6300 to 7000 cm^{-1}, J. Quant. Spectrosc. Radiat. Transfer 113 (2012) 1066-1083.

HNO_3 (molecule 13)

GEISA-2015 includes, for the first time, a line list at 11.2 μm for the second-most abundant isotopologue of nitric acid, $H^{15}NO_3$ with a $^{15}N/^{14}N$ natural isotopic ratio of approximately 0.00365(7). The ν_5 and $2\nu_9$ vibrational bands for this isotopologue were added using a high resolution Fourier transform investigation performed at 11 μm by Perrin and Mbiaké **[1]**.

However since the resonance coupling the ν_5 and $2\nu_9$ energy levels is significantly weaker for $H^{15}NO_3$ than for $H^{14}NO_3$, the intensity transfer from the fundamental (and in principle strong) ν_5 band to the overtone (and in principle weak) $2\nu_9$ band is significantly weaker for $H^{15}NO_3$ than for $H^{14}NO_3$. Therefore in GEISA-2015 the $H^{15}NO_3$ and $H^{14}NO_3$ ν_5 bands are in an intensity ratio which is about ~1.4 larger than the expected value assumed from the $^{15}N/^{14}N$ natural isotopic ratio. Finally the air- and self-broadened half widths and temperature dependence were adopted from the work of Flaud et al. **[2]**.

Fig. 1 gives an overview of the ν_5 and $2\nu_9$ bands of $H^{14}NO_3$ and $H^{15}NO_3$. One can see that the narrow Q branch structure of the ν_5 band of $H^{15}NO_3$ is shifted to the low frequency range (at about 871 cm^{-1}) compared to its $H^{14}NO_3$ counterpart (at about 879 cm^{-1}).

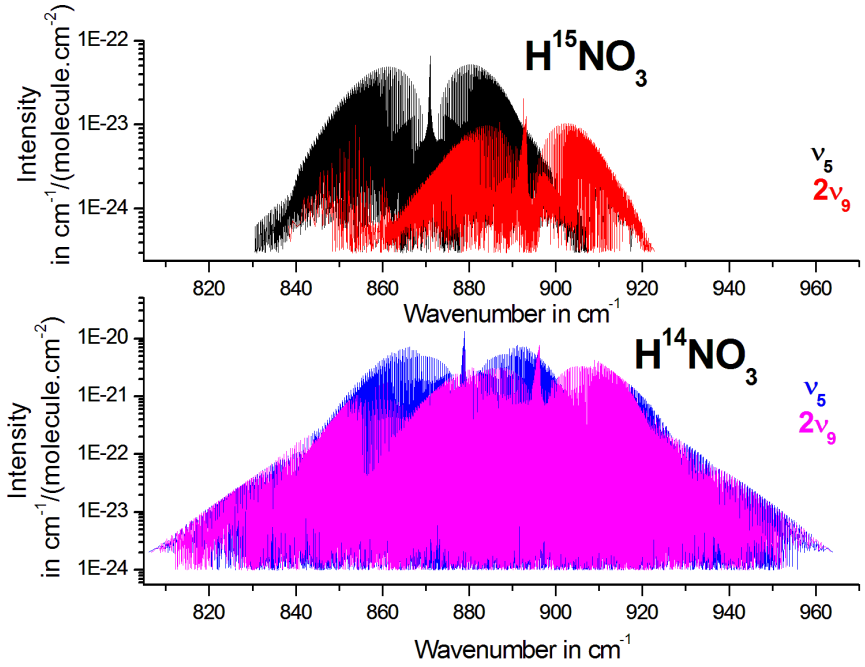

Fig.1. Graphical overview of the ν_5 and $2\nu_9$ cold bands for $H^{14}NO_3$ and $H^{15}NO_3$.

The evidence of the ν_5 spectral signature of $H^{15}NO_3$ showed in the atmospheric limb-emission spectra measured by MIPAS **[3]**. Later, this signature was used to report the first measurement of the isotopic partitioning between stratospheric $H^{14}NO_3$ and $H^{15}NO_3$ **[4].**

Table 1 gives an overview of the GEISA-2015 entry for nitric acid in the 11 µm region, for both isotopologues $H^{14}NO_3$ (Part A) and $H^{15}NO_3$ (part B).

Table 1
Overview of the GEISA-2015 entry for nitric acid in the 11 µm region. The upper and lower vibrational identifications of actual transitions are given in columns 1 and 2 respectively; for each transition: the total number of lines, the total intensity (in cm molecule^{-1} at 296 K), the minimum and maximum wavenumber of the lines, as well as the minimum and maximum intensity (in cm molecule^{-1} at 296 K), are in columns 3 to 8, respectively.

A) $H^{14}NO_3$

Vib'	Vib"	# lines	Total Int. (cm molecule^{-1}) at 296 K	Wavenumber min (cm^{-1})	Wavenumber max (cm^{-1})	Int._min. (cm molecule^{-1}) at 296 K	Int._max. (cm molecule^{-1}) at 296 K
ν_5	GS	57,108	0.1027 X 10^{-16}	806.207	963.995	0.983 X 10^{-24}	0.660 X 10^{-20}
$2\nu_9$	GS	55,310	0.7503 X 10^{-17}	806.709	963.435	0.983 X 10^{-24}	0.388 X 10^{-20}
$3\nu_9$	ν_9	17,720	0.5291 X 10^{-18}	769.687	884.438	0.384 X 10^{-24}	0.672 X 10^{-21}
$\nu_5+\nu_6$	ν_6	57,108	0.6179 X 10^{-18}	796.207	953.995	0.592 X 10^{-25}	0.397 X 10^{-21}

Vib'	Vib"	# lines	Total Int. (cm molecule^{-1}) at 296 K	Wavenumber min (cm^{-1})	Wavenumber max (cm^{-1})	Int._min. (cm molecule^{-1}) at 296 K	Int._max. (cm molecule^{-1}) at 296 K
$\nu_5+\nu_7$	ν_7	57108	0.9761 X 10^{-18}	802.807	960.595	0.935 X 10^{-25}	0.627 X 10^{-21}
$\nu_5+\nu_9$	ν_9	14521	0.1068 X 10^{-17}	832.116	942.901	0.987 X 10^{-24}	0.700 X 10^{-21}

B) $H^{15}NO_3$

Vib'	Vib"	# lines	Total Int. (cm molecule^{-1}) at 296 K	Wavenumber min (cm^{-1})	Wavenumber max (cm^{-1})	Int._min. (cm molecule^{-1}) at 296 K	Int_max (cm molecule^{-1}) at 296 K
ν_5	GS	12883	0.5023 X 10^{-19}	830.371	919.725	0.300 X 10^{-24}	0.330 X 10^{-22}
$2\nu_9$	GS	8290	0.9917 X 10^{-20}	838.223	922.931	0.300 X 10^{-24}	0.625 X 10^{-23}

References

[1] A. Perrin and R. Mbiaké, The ν_5 and $2\nu_9$ bands of the ^{15}N isotopic species of nitric acid ($H^{15}NO_3$): Line positions and intensities, J. Molec. Spectrosc. 237 (2006) 27-35

[2] J-M. Flaud, G. Brizzi, M. Carlotti, A. Perrin, M. Ridolfi, MIPAS database: validation of HNO_3 line parameters using MIPAS satellite measurements, Atmos. Chem. Phys. 6 (2006) 5037–5048.

[3] G. Brizzi, M. Carlotti, J-M. Flaud, A. Perrin and M. Ridolfi. First observation of $H^{15}NO_3$ in atmospheric spectra, Geophys. Res. Lett. 34 (2007) L038025.

[4] G. Brizzi, E. Arnone, M. Carlotti, B.M. Dinelli, J.-M. Flaud, E. Papandrea, A. Perrin and M. Ridolfi. Retrieval of atmospheric $H^{15}NO_3$/ $H^{14}NO_3$ isotope ratio profile from MIPAS/ENVISAT limb measurements, J. Geophys. Res. 114 (2009) doi:10.1029/2008JD011504

H_2CO (molecule 21)

Formaldehyde has been completely revised in the microwave and far infrared using the line list of positions and intensities from the CDMS database for the three isotopologues present in GEISA, namely $H_2{}^{12}C^{16}O$, $H_2{}^{12}C^{18}O$, and $H_2{}^{13}C^{16}O$. Whereas GEISA-2011 had 1541 lines for these isotopologues ranging from 0 to 100 cm^{-1}, 9102 transitions are now present in GEISA-2015, between 0 and 508 cm^{-1}.

Three H_2CO isotopologue data implemented in GEISA-2015, i.e. (as identified in the CDMS catalog) is:

30501.cat (H_2CO-16) 5171 entries ($H_2{}^{12}C^{16}O$)

32503.cat (H_2CO-18) 1622 entries ($H_2{}^{12}C^{18}O$)

31503.cat (H_2C-13-O) 2309 entries ($H_2{}^{13}C^{16}O$)

These new data totally replace the previous entries.

The self-widths, air-widths and temperature dependence of the air-widths have been updated using the calculated values of Jacquemart et al. **[1]** for the whole three isotopologue line lists.

The data should be viewed with some caution at temperatures much higher than 300 K.

Reference

[**1**] D. Jacquemart, F. Kwabia Tchana, N. Lacome, A. Perrin, A. Laraia, R.R. Gamache, Formaldehyde around 3.5 and 5.7-μm: measurement and calculation of broadening coefficients, J. Quant. Spectrosc. Radiat. Transfer 111 (2010) 1209–1222.

C_2H_6 (molecule 22)

In GEISA-2015, $^{12}C_2H_6$ line parameters are available for three wavelengths: 12 µm, 7 µm and 3.3 µm, **[1,2,3]**, and the ν_{12} band of $^{12}CH_3{}^{13}CH_3$ at 12 µm **[4]**.

At 12 µm, previous calculated line parameters for the ν_9 fundamental, the $3\nu_4$ overtone and two hot bands were retained with adjustments to specific line parameters. New line shape measurements by Devi et al. **[2,3]** permitted derived empirical expressions for self- and N_2-broadened line shapes and their temperature dependence to be applied assuming $\gamma_{air} = 0.9 \times \gamma_{N2}$; the calculated line intensities **[5]** were reduced by 15% as well.

At 7 µm, the ethane spectrum is dominated by the ν_6 and ν_8 fundamental bands, and these have proved useful for the analyses of the Titan atmosphere. Line parameters for $^{12}C_2H_6$ were added **[6]**.

At 3.3 µm, the highest ethane fundamental band ν_7 is overlapped by numerous overtone and combination states, making it difficult to provide reliable ethane spectroscopy for remote sensing. For GEISA-2015 the work of Lattanzi et al. **[7]** was used because it provides the most extensive modeling of direct measurements for this region.

References

[**1**] L.S. Rothman et al. (2009). The HITRAN 2008 molecular spectroscopic database. J. Quant. Spectrosc. Radiat. Transfer, Vol. 110, pp. 533–572. doi: 10.1016/j.jqsrt.2009.02.013.

[2] V.M. Devi, C.P. Rinsland D.C. Benner, R. L. Sams, T. A. Blake, Multispectrum analysis of the ν_9 band of $^{12}C_2H_6$: Positions, intensities, self- and N_2-broadened half-width coefficients, J. Quant. Spectrosc. Radiat. Transfer 111 (2010) 1234-51.

[**3]** V.M. Devi, D.C. Benner, C.P. Rinsland, M. A. H. Smith, R. L. Sams, T. A. Blake, J.-M. Flaud, K. Sung, L.R. Brown, A.W. Mantz, Multispectrum measurements of spectral line parameters including temperature dependences of N_2- and self-broadened half-width coefficients in the region of the ν_9 band of $^{12}C_2H_6$, J. Quant. Spectrosc. Radiat. Transfer 111 (2010) 2481-2504.

[4] V.M. Devi, D.C. Benner, K. Sung, T.J. Crawford, A.W. Mantz, Line positions and intensities for the ν_{12} band of $^{13}C^{12}CH_6$, J. Molec.Spectrosc. 301 (2014) 28–38.

[5] L.S. Rothman, I.E. Gordon, Y. Babikov, A. Barbe, D. Chris Benner, P.F. Bernath, M. Birk, L. Bizzocchi, V. Boudon, L.R. Brown, A. Campargue, K. Chance, E.A. Cohen, L.H. Coudert, V.M. Devi, B.J. Drouin, A. Fayt, J.-M. Flaud, R.R. Gamache, J.J. Harrison, J.-M. Hartmann, C. Hill, J.T. Hodges, D. Jacquemart, A. Jolly, J. Lamouroux, R.J. Le Roy, G. Li, D.A. Long, O.M. Lyulin, C.J. Mackie, S.T. Massie, S. Mikhailenko, H.S.P. Müller, O.V. Naumenko, A.V. Nikitin, J. Orphal, V. Perevalov, A. Perrin, E.R. Polovtseva, C. Richard, M.A.H. Smith, E. Starikova, K. Sung, S. Tashkun, J. Tennyson, G.C. Toon, Vl.G. Tyuterev, G. Wagner (2013). The HITRAN 2012 molecular spectroscopic database. J. Quant. Spectrosc. Radiat. Transfer Vol. 130, 4–50. doi: 10.1016/j.jqsrt.2013.07.002.

[6] N. Moazzen-Ahmadi, J. Norooz Oliaee, I. Ozier, E. H. Wishnow, K. Sung, T. Crawford, L. R. Brown, V. M. Devi, An intensity study of the torsional bands of ethane at 35 μm, J. Quant. Spectrosc. Radiat. Transfer 151 (2015) 123–132.

[7] F. Lattanzi, C. di Lauro, J. Vander Auwera, Toward the understanding of the high resolution infrared spectrum of C_2H_6 near 3.3 μm, J. Molec.Spectrosc. 267 (2011) 71-79.

CH_3D (molecule 23)

The GEISA-2015 CH_3D database been updated in 2 spectral regions:

- In the spectral region between 4000 cm^{-1} and 4550 cm^{-1}, over 4000 lines of $^{12}CH_3D$ were included for the first time **[1]**. Measured line positions and intensities for nine new bands of the Enneadecad polyad were obtained using high resolution FTIR spectra recorded using enriched gas samples (98% D) at room and cold (80 K) temperatures. To construct a new line list, many lower state energies were determined from quantum assignments, and confirmed by effective Hamiltonian and dipole moment expansion models. For pressure broadening coefficients, empirical expressions based on measurements of CH_3D bands near 7 μm **[2,3]** and the references therein were applied as a function of known quantum numbers to approximately represent the air- and self-broadened half widths and pressure-induced shifts. Additional details are given in Ref. **[4]**.

-In the 6204.025190-6510.324200 cm^{-1} region, the position and intensity values of 5692 newly-included lines are taken from the supplementary material of Lu et al. **[5].**

References

[1] A.V. Nikitin, L. R. Brown, M. Rey, Vl. G. Tyuterev, K. Sung, M. A. H. Smith, A.W. Mantz. Preliminary modeling of CH_3D from 4000 to 4550 cm^{-1}. J. Quant. Spectrosc. Radiat. Transfer 114 (2013) 1-12.

[2] V.M. Devi, D.C. Benner, MAH Smith, C.P. Rinsland , Measurements of air broadened width and air induced shift coefficients and line mixing in the v_5 band of $^{12}CH_3D$, J. Quant. Spectrosc. Radiat. Transfer 68 (2001) 135-161.

[3] V.M. Devi, D.C. Benner, MAH Smith, C.P. Rinsland, L.R. Brown, Self- and nitrogen- broadening, pressure induced shift and line mixing coefficients in the v_5 of $^{12}CH_3D$ using a multi-spectrum fitting procedure, J. Quant. Spectrosc. Radiat. Transfer 74 (2002)1-41.

[4] L. R. Brown, K. Sung, D. C. Benner, V. M. Devi, V. Boudon, T. Gabard, C. Wenger, A. Campargue, O. Leshchishina, S. Kassi, D. Mondelain, L. Wang, L. Daumont, L. Régalia, M. Rey, X. Thomas, Vl. G. Tyuterev, O. M. Lyulin, A. V. Nikitin, H. M. Niederer, S. Albert, S. Bauerecker , M. Quack, I. E. Gordon, L. S. Rothman, H. Sasada, A. Coustenis, M. A. H. Smith, T. Carrington Jr., X. G. Wang, A. W. Mantz, P. T.

Spickler, Methane line parameters in the HITRAN 2012 database, J. Quant. Spectrosc. Radiat. Transfer 130 (2013) 201-219.

[5] Y.Lu, D. Mondelain, S. Kassi and A.Campargue, The CH3D absorption spectrum in the 1.58 micron transparency window of methane :empirical line lists and temperature dependence between 81K and 294K, J. Quant. Spectrosc. Radiat. Transfer 112 (2011) 2683-2697.

C_2H_2 (molecule 24)

In the 7.7 µm region, acetylene absorbs mainly at room temperature via the strong cold band $(\upsilon_4 - \upsilon_5)^0_+$ for which spectroscopic parameters **[1]** were previously available in databases **[2,3]**. This spectral region was used in 2006 **[4]** to observe acetylene signatures in carbon-rich asymptotic giant branch stars but the lack of spectroscopic data in this region did not allow the observation to be correctly reproduced. The temperature of interest for applications being around 500 K **[4]**, the spectroscopic information for hot bands is also important. In the recent work from Gomez et al. **[5,6]**, a complete line list of 2 cold bands (including the band $(\upsilon_4 - \upsilon_5)^0_+$) and 15 hot bands has been generated and has been used to update the 7.7µm region of GEISA-2015. This line list of 1629 transitions between 1142 and 1451 cm^{-1} replaced the previous 71 transitions of the $(\upsilon_4 - \upsilon_5)^0_+$ band between 1248 and 1415 cm^{-1}.

References

[1] J. Vander Auwera, Absolute intensities measurements in the the $(\nu_4 - \nu_5)$ band of $^{12}C_2H_2$: analysis of Herman–Wallis effects and forbidden transitions, J. Mol. Spectrosc. 201 (2000) 143–150.

2] N. Jacquinet-Husson, N.A. Scott, A. Chédin, K. Garceran, R. Armante, A.A. Chursin et al., The 2003 Edition of the GEISA/IASI spectroscopic database, J. Quant. Spectrosc. Radiat. Transfer 95 (2005) 429-467.

[3] L.S. Rothman et al., The HITRAN 2004 molecular spectroscopic database. J. Quant. Spectrosc. Radiat. Transfer 96 (2005)139-204.

[4] M. Matsuura, P.R. Wood, G.C. Sloan, A.A. Zijlstra, J.T. van Loon, M.A.T. Groenewegen, et al., Spitzer observations of acetylene bands in carbon-rich asymptotic giant branch stars in the Large Magellanic Cloud, Mon. Not. Roy. Astron. Soc. 371 (2006) 415–420.

[5] L. Gomez, D. Jacquemart, N. Lacome, J.-Y. Mandin, Line intensities of $^{12}C_2H_2$ in the7.7 µm spectral region, J. Quant. Spectrosc. Radiat. Transfer 110 (2009) 2102–2114.

[6] L. Gomez, D. Jacquemart, N. Lacome, J.-Y. Mandin, New line intensity measurements for $^{12}C_2H_2$ around 7.7 µm and HITRAN format line list for applications, J. Quant. Spectrosc. Radiat. Transfer 111 (2010) 2256–2264.

C_2H_4 (molecule 25)

New spectroscopic line parameters for ethylene included in GEISA-2015 concern both the main isotopologue, $^{12}C^{12}CH_4$ and the less abundant $^{12}C^{13}CH_4$ isotopologue. More precisely the new line

list contains 9 bands: $\nu_8+\nu_{10}$, $\nu_7+\nu_8$, $\nu_4+\nu_8$, $\nu_8+\nu_{12}$, $\nu_6+\nu_{10}$, $\nu_6+\nu_7$, $\nu_4+\nu_6$, $\nu_3+\nu_{10}$, $\nu_3+\nu_7$ of the main isotopologue $^{12}C^{12}CH_4$ covering the spectral region 1656-2487 cm^{-1} **[1,2]** and 5 bands: ν_{10}, ν_8, ν_7, ν_4, ν_6 for $^{12}C^{13}CH_4$ covering the spectral region 615-1339 cm^{-1} **[3,4]**.

In the absence of measurements or calculations for the line-shape parameters, default values were chosen, i.e.:

HWHM γ_{air} = 0.0870 $cm^{-1}atm^{-1}$ at 296 K

HWHMself γ_{self} = 0.1245 $cm^{-1}atm^{-1}$ at 296 K

Temperature-dependence coefficient *n* of the air broadening half width n_{air} =0.82

The GEISA standard default value, δ_{air} = 0.000000 $cm^{-1}atm^{-1}$ at 296 K, is used for the air pressure induced shift of the line transition.

The GEISA-2015 C_2H_4 updated file contains 53,227 entries (18,378 in GEISA-2011), corresponding to a total of 26 vibrational bands (12 in GEISA-2011).

References

[1] W.J. Lafferty, J.-M. Flaud, F. Kwabia Tchana, The high-resolution infrared spectrum of ethylene in the 1800–2350 cm^{-1} spectral region, Molec. Phys.. 109:21(2011) 2501-2510.

[2] A. Ben Hassen, F. Kwabia Tchana, J.-M. Flaud, W.J. Lafferty, X. Landsheere, H. Aroui, Absolute line intensities for ethylene from 1800 to 2350 cm^{-1}, J. Molec. Spectrosc. 282 (2012) 30–33.

[3] J.-M. Flaud, W.J. Lafferty, Robert Sams, V. Malathy Devi, High resolution analysis of the ethylene-1-^{13}C spectrum in the 8.4–14.3-μm region, J. Molec. Spectrosc. 259 (2010) 39–45.

[4] J.-M. Flaud, W.J. Laffert , V. Malathy Devi, R.L. Sams, D. Chris Benner, Absolute line intensities and self-broadened half-width coefficients in the ethylene-1-^{13}C bands in the 700–1190 cm^{-1} region, J. Molec. Spectrosc. 267 (2011) 3–12.

HCN (molecule 27)

Over the last few years Mellau **[1,2]** has performed emission experiments on hot HCN. Using Mellau's energy levels and the *ab-initio* line intensities computed by Harris et al. **[3],** Barber et al. **[4]** built up an extensive database of experimental HCN energy levels. This line list was designed for studies of hot astronomical problems and contains hundreds of millions of lines. For present purposes a 296 K $H^{12}C^{14}N$ line list was generated and only the 131,139 lines stronger than 10^{-31} were retained to form the input for GEISA-2015. In the spectral range 9933.825951-17581.009367 cm^{-1}, 4871 lines from Harris have been kept from GEISA-2011 **[5]**; 2085 experimentally-measured lines from Maki **[5]**, in the region 2.415494-3550.842326 cm^{-1}, have been kept from GEISA-2011, alongside data for the 3 other isotopologues: $H^{13}C^{15}N$, $H^{13}C^{14}N$, $D^{12}C^{14}N$.

The update file provided by UCL contained no line shape parameters. The missing parameters were therefore created using the GEISA-2011 HCN ones for lines with a similar

quantum identification. For the other lines, the default values were attributed as follows:

HWHM γ_{air} = 0.1011 $cm^{-1}atm^{-1}$ at 296 K

HWHMself γ_{self} = 0.1245 $cm^{-1}atm^{-1}$ at 296 K

Temperature-dependence coefficient *n* of the air broadening half width n_{air} =0.70

The GEISA standard default value, δ_{air} = 0.000000 $cm^{-1}atm^{-1}$ at 296 K, was used for the air pressure induced shift of the line transition.

The GEISA-2015 HCN line list contains a total of 138,103 entries (81,889 in GEISA-2011).

References

[1] G.C. Mellau, Complete experimental rovibrational eigen energies of HCN up to 6880 cm^{-1} above the ground state, J. Chem. Phys. 134 (2011), 234-303.

[2] G.C. Mellau, Rovibrational eigen energy structure of the H,C,N molecular system, J. Chem. Phys. 134 (2011) 194-302.

[3] G.J. Harris, O.L. Polyansky and J. Tennyson, Opacity data for HCN and HNC from a new ab initio linelist, Astrophys. J. 578 (2002) 657-663.

[4] R.J. Barber, J. Strange, C. Hill, O.L. Polyansky, G. Mellau, S.N. Yurchenko and J. Tennyson, ExoMol Molecular linelists: III An improved hot rotation-vibration line list for HCN and HNC, Mon. Not. Roy. Astron. Soc. 437 (2014) 1828-1835.

[5] N. Jacquinet-Husson, L. Crepeau, R. Armante, C. Boutammine, A. Chédin, N.A. Scott, C. Crevoisier , V. Capelle, C. Boone, N. Poulet-Crovisier, A. Barbe, A. Campargue, D. Chris Benner, Y. Benilan, B. Bézard, V. Boudon, L.R. Brown, L.H. Coudert, A. Coustenis, V. Dana, V.M. Devi, S. Fally, A. Fayt, J.-M Flaud, A. Goldman, M. Herman, G.J. Harris, D. Jacquemart, A. Jolly, I. Kleiner, A. Kleinböhl, F. Kwabia-Tchana, N. Lavrentieva, N. Lacome, Li-Hong Xu, O.M. Lyulin, J.-Y. Mandin, A. Maki, S. Mikhailenko, C.E. Miller, T. Mishina, N. Moazzen-Ahmadi, H.S.P. Müller, A. Nikitin, J. Orphal, V. Perevalov, A. Perrin, D.T. Petkie, A. Predoi-Cross, C.P. Rinsland, J.J. Remedios, M. Rotger, M.A.H. Smith, K. Sung, S. Tashkun, J. Tennyson, R.A. Toth, A.-C. Vandaele, J. Vander Auwera, The 2009 edition of the GEISA spectroscopic database. J. Quant. Spectrosc. Radiat. Transfer 112 (2011) 2395–2445. doi: 10.1016/j.jqsrt. 2011.06.004.

C_2N_2 (molecule 29)

The $^{12}C_2{}^{14}N_2$ (cyanogen) line list in GEISA-2011 included 2577 entries mainly belonging to the ν_5 bending system centered at 234 cm^{-1} and also lines from the weak stretching ν_2 mode around 2150 cm^{-1}. In GEISA-2015, all the entries belonging to ν_5 have been replaced by a new line list based on experimental and theoretical work by Fayt et al. **[1]**. This new study includes a recording of the high resolution spectrum and the first ro-vibrational global analysis for this molecule. The positions of about 13000 peaks were obtained experimentally and analyzed to determine very accurate molecular parameters..

Spectra of C_2N_2 at low resolution were also recorded (Fayt et al. **[1]**) in order to determine the band system intensity.

The updated GEISA-2015 $^{12}C_2{}^{14}N_2$ line list involves a total of 71,774 entries (only 181 kept from the former editions).

Reference

[1] A. Fayt, A. Jolly, Y. Benilan, L. Manceron, F. Kwabia-Tchana, J.-C. Guillemin, Frequency and intensity analysis of the far infrared ν_5 band complex of cyanogen (C_2N_2) and applications to Titan, J. Quant. Spectrosc. Radiat. Transfer 113 (2012) 1195-1219.

C_4H_2 (molecule 30)

The line list of C_4H_2 in GEISA-2011 (119,480 entries) was based on preliminary results from the global ro-vibrational analysis of both bending modes ν_8 (628.0 cm^{-1}) and ν_9 (220.1 cm^{-1}) described in Jolly et al. **[1]**. GEISA-2015 includes the final version of this line list. The number of lines (417,540) is much larger than in GEISA-2011 because the calculation includes the contribution of hot bands, up to the polyad containing $9\nu_9 \leftarrow 8\nu_9$, corresponding to a maximum vibrational energy level of the lower state E"=1700 cm^{-1}. The intensity of all the transitions belonging to the analyzed polyads are calculated and included in the line list if the intensity at room temperature is stronger than a cut-off value of about 10^{-7} times the band intensity.

In addition to the lines from the two bending modes already present in GEISA-2011, new lines from the strong combination band $\nu_6+ \nu_8$ at 1240.7 cm^{-1} have been included in GEISA-2015. The line list of $\nu_6+\nu_8$ was calculated based on the very accurate results of a global analysis which enables parameters for vibrational levels with high energies including combination levels to be determined.

One major update in GEISA-2015 concerns the intensities of the ν_8 and ν_9 bands. While the band intensities in GEISA-2011 relied on measurements madeby Koops et al. **[2]**, the new version relies on recent measurements by Jolly et al. **[3],** who find large differences compared to Koop et al.'s values, in particular for the ν_9 band and for the ν_8 and $\nu_6+ \nu_8$ combination band, as well, for which the result obtained by Jolly et al. **[3]** confirmed the previous measurement by Khlifi et al. **[4]**.

References

[1] A. Jolly, A. Fayt, Y. Benilan, D. Jacquemart, C.A. Nixon, D.E. Jennings, The ν_8 bending mode of diacetylene: from laboratory spectroscopy to the detection of ^{13}C isotopologues in Titan's atmosphere, Astrophys. J. 714 (2010) 852-859.

[2] T. Koops, T. Visser, W.M.A. Smit, The harmonic force field and absolute infrared intensities of diacetylene, J. Molec. Struct. 125 (1984) 179-196.

[3] A. Jolly, L. Manceron, F. Kwabia-Tchana, Y. Benilan, M-C. Gazeau, Revised infrared bending mode intensities for diacetylene (C_4H_2): application to Titan, Planetary and Space Sciences 97 (2014) 60-64.

[4] M. Khlifi, P. Paillous, C. Delpech, M. Nishio, P. Bruston, F. Raulin, Absolute IR band intensities of diacetylene in the 250-4300 cm^{-1} region - implications for Titan's atmosphere, J. Molec. Spectrosc. 174 (1995) 116-122.

CH_3Cl (molecule 34)

The methyl chloride line list is completely updated in GEISA-2015 on the basis of various works, depending on the spectral regions and on the line parameters.

Line positions and intensities from JPL catalog **[1,2]** are used between 0.8 and 71 cm^{-1} (12,824 pure rotational transitions).

Between 644 and 2625 cm^{-1}, a calculation by Nikitin based on effective Hamiltonian has been used for positions **[3,4]**. As this calculation provides absolute line positions but only approximate relative line intensities **[4]**, a calibration based on measurements has been performed to retrieve absolute intensity values. Finally, 46,406 transitions calculated from Ref. **[3]** and belonging to the fundamental bands ν_3, ν_6, ν_2 and ν_5 are introduced in GEISA-2015.

Between 2920 and 3198 cm^{-1}, line positions and intensities of 22,963 transitions in the 3 μm region from Bray el al. **[5]** are used. These transitions mainly concern the strong fundamental band ν_1, but some of them refer to the weaker ν_4 band or other harmonic or combination bands.

The semi-empirical calculations by Dudaryonok et al. **[6]** for the $CH_3{}^{35}Cl$ self-broadening case and the semi-classical calculations of Buldyreva **[7]** for the $CH_3{}^{35}Cl$ and $CH_3{}^{37}Cl$ air-broadening case, providing the broadening coefficients for the reference temperature 296 K and the associated temperature exponents, are used for all transitions listed in the database.

References

[1] H.M. Pickett, R.L. Poynter, E.A. Cohen, M.L. Delitsky, J.C. Pearson H.S.P. Müller, Submillimeter, millimeter, and microwave spectral line catalog, J. Quant. Spectrosc. Radiat. Transfer 60 (1998) 883–890.

[2] J.C. Pearson, H.S.P. Müller, H.M. Pickett, E.A. Cohen B.J. Drouin, Introduction to submillimeter, millimeter and microwave spectral line catalog, J. Quant. Spectrosc. Radiat. Transfer 111 (2010) 1614–1616.

[3] A.V. Nikitin, J.-P. Champion, New ground state constants of $^{12}CH_3{}^{35}Cl$ and $^{12}CH_3{}^{37}Cl$ from global polyad analysis, J. Molec. Spectrosc. 230 (2005) 168–173.

[4] A.V. Nikitin, J.-P. Champion, H. Bürger, Global analysis of $^{12}CH_3{}^{35}Cl$ and $^{12}CH_3{}^{37}Cl$: simultaneous fit of the lower five polyads (0–2600 cm^{-1}), J. Molec. Spectrosc. 230 (2005) 174–184.

[5] C. Bray, A. Perrin, D. Jacquemart, N. Lacome, The ν_1, ν_4 and $3\nu_6$ bands of methyl chloride in the 3.4 μm region: Line positions and intensities, J. Quant. Spectrosc. Radiat. Transfer 112 (2011) 2446–2462.

[6] A.S. Dudaryonok, N.N. Lavrentieva, J. Buldyreva, CH_3Cl self-broadening coefficients and their temperature dependences, J. Quant. Spectrosc. Radiat. Transfer 130 (2013) 321–326.

[7] J. Buldyreva, Air-broadening coefficients of $CH_3{}^{35}Cl$ and $CH_3{}^{37}Cl$ rovibrational lines and their temperature dependence by a semi-classical approach, J. Quant. Spectrosc. Radiat. Transfer 130 (2013) 315–320.

H_2S (molecule 36)

A very significant update of the H_2S data is implemented in GEISA–2015 to provide 58,650 transitions of the three isotopic species, $H_2{}^{32}S$, $H_2{}^{33}S$, $H_2{}^{34}S$. This represents an increase of 37,862 lines compared to GEISA-2011 **[1]** (20,788 lines). The new or updated transitions fall within four spectral ranges: 1.0–615 cm^{-1}, 994–1574 cm^{-1}, 2143–4257 cm^{-1}, and 4472–113201 cm^{-1}.

Pure rotational transitions of hydrogen sulfide in its ground and first excited vibrational states between 1.03056–614.89397 cm^{-1} were recorded at room temperature by Azzam et al. **[2]**. The line positions given in their Supplementary data have been applied to 8430 transitions, formerly represented by 3396 lines in GEISA-2011.

Updated positions for the ν_2 region (994.1296–1573.8098 cm^{-1}): for the 010–000 band, line positions of 653 transitions from GEISA-2011 were improved **[3]** using experimental upper energy levels for $H_2{}^{32}S$, $H_2{}^{33}S$, and $H_2{}^{34}S$ isotopologues reported by Ulenikov et al. **[4]**; the lower energy levels were calculated using the rotational constants of Flaud et al. **[5]**.

Fig. 1 shows that, in GEISA-2015, the ν_2 band positions are clearly shifted by ~ 0.002 cm^{-1}, with a maximum difference reaching to 0.055 cm^{-1}, compared to HITRAN-2012 **[6]**. The precision obtained is estimated to be about 0.0002 cm^{-1}. These corrections were not reported in HITRAN-2012. The calculated transition intensities are the same as in GEISA-2011 and HITRAN-2012.

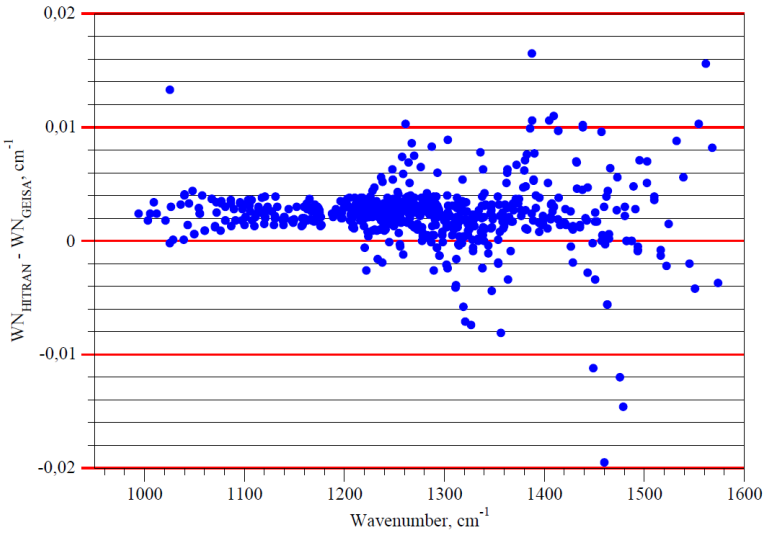

Fig. 1 Comparison of the 010-000 band updated lines in GEISA-2015 with those of HITRAN-2012 illustrating differences in wavenumber (WN) positions (WN_{HITRAN}-WN_{GEISA} (cm^{-1})).

Updates in the 2142.83505–4256.54681 cm^{-1} spectral region cover bands of the first and second triads. O. Naumenko generated a corrected file **[3]** including 16,731 entries which have replaced, in GEISA-2015, the former GEISA-2011 data.

New parameters were added in the spectral region 4471.7721–11329.7799 cm^{-1}, this spectral region covers the first and second hexads along part of the first decade of H_2S. It is included for the first time in GEISA using 28,972 transitions of $H_2{}^{32}S$, $H_2{}^{33}S$, and $H_2{}^{34}S$ from Ref. **[3]**. The information newly included in GEISA-2015 relates to 30 vibrational bands of $H_2{}^{32}S$ and is summarized in the 8 columns of Table 1.

In total, 16284, 4087 and 1666 transitions of isotopologues $H_2{}^{32}S$, $H_2{}^{34}S$, and $H_2{}^{33}S$, respectively, have been newly implemented in GEISA-2015 between 4471.772110 and 8039.744310 cm^{-1}.

The line shape parameters are those reported in HITRAN-2012.

Table 1

New vibrational bands of $H_2{}^{32}S$ included in GEISA-2015. For each vibrational band: the quantum identifications of the upper and lower levels of the transition, in the two first columns; the extension of the spectral region from WN min (minimum wave number in cm^{-1},) to WN max (maximum wave number in cm^{-1} molecule^{-1}), in columns 3 and 4 respectively; the summed transition intensities in cm, in column 5; the maximum values of the rotational quantum numbers J and K_a, in columns 7 and 8 respectively; the number of transitions is given in the last column.

$V_1V_2V_3$ Upper	$V_1V_2V_3$ Lower	WN_min (cm^{-1})	WN_max (cm^{-1})	∑int (cm molecule^{-1}) at 296 K	J_max Upper	K_a_max Upper	# lines
040	000	4471.7721	5094.0399	7.22×10^{-23}	16	8	535
021	000	4555.7922	5392.1073	2.17×10^{-21}	19	12	1169
101	000	4647.9645	5545.0965	2.59×10^{-20}	20	12	1886
200	000	4676.6355	5548.5630	1.25×10^{-20}	19	14	1636
120	000	4720.3837	5387.7404	7.41×10^{-22}	16	12	844
002	000	4828.3805	5665.5575	2.51×10^{-21}	18	13	1220
111	010	4877.2258	5240.4972	1.16×10^{-22}	15	10	403
210	010	4889.8533	5249.6706	5.03×10^{-23}	15	9	326
050	000	5671.4441	6029.4104	9.91×10^{-24}	12	5	203
130	000	5840.1421	6579.5353	1.38×10^{-22}	15	9	566
031	000	5844.5832	6582.2596	1.30×10^{-22}	16	10	541
111	000	5887.1896	6695.2663	1.13×10^{-20}	18	13	1423
210	000	5984.9635	6693.3914	2.95×10^{-21}	18	14	1484
012	000	5989.3819	6664.1874	5.21×10^{-23}	13	9	126
121	010	6051.8265	6489.7069	6.91×10^{-23}	14	8	380
220	010	6071.8079	6477.5959	2.71×10^{-23}	12	7	198
121	000	7053.2468	7738.0455	1.89×10^{-22}	14	8	539
220	000	7128.4865	7672.2512	1.77×10^{-23}	12	7	248
201	000	7170.3630	7868.6880	7.78×10^{-22}	17	10	794
102	000	7191.1311	7766.3336	2.32×10^{-22}	13	10	601
300	000	7400.1750	8039.7443	2.80×10^{-22}	14	9	601
003	000	7496.6411	8031.1830	1.86×10^{-22}	14	9	560
141	000	9385.1150	9991.9363	7.23×10^{-25}	12	8	385
122	000	9470.6934	10157.4780	2.24×10^{-24}	15	8	492
301	000	9477.0610	10241.6542	3.10×10^{-23}	16	11	1074
221	000	9494.1657	10154.2523	4.97×10^{-24}	15	10	656
202	000	9528.5303	10266.7543	9.98×10^{-24}	18	9	840
212	000	10777.8636	11329.7798	1.49×10^{-23}	19	11	996
311	000	10777.8636	11317.3960	2.26×10^{-23}	19	11	902
330	000	10948.4353	11278.5380	3.82×10^{-25}	10	7	232

ICLAS and ICLAS-VECSEL systems were used to probe the weak H_2S absorption spectrum in the 9385-10200 cm^{-1} **[7]** and 10780-11330 cm^{-1} **[7]** spectral regions. Spectra were obtained from transitions to the eight highly-excited upper vibrational states listed in Table1. In total, 5605, 1185 and 146 new transitions of isotopologues $H_2{}^{32}S$, $H_2{}^{34}S$, and $H_2{}^{33}S$, respectively, have been included in GEISA-2015 between 9385.115080 and 11329.779860 cm^{-1}.

References

[1] N. Jacquinet-Husson, L. Crepeau, R. Armante, C. Boutammine, A. Chédin, N.A. Scott, C. Crevoisier , V. Capelle, C. Boone, N. Poulet-Crovisier, A. Barbe, A. Campargue, D. Chris Benner, Y. Benilan, B. Bézard, V. Boudon, L.R. Brown, L.H. Coudert, A. Coustenis, V. Dana, V.M. Devi, S. Fally, A. Fayt, J.-M Flaud, A. Goldman, M. Herman, G.J. Harris, D. Jacquemart, A. Jolly, I. Kleiner, A. Kleinböhl, F. Kwabia-Tchana, N. Lavrentieva, N. Lacome, Li-Hong Xu, O.M. Lyulin, J.-Y. Mandin, A. Maki, S. Mikhailenko, C.E. Miller, T. Mishina, N. Moazzen-Ahmadi, H.S.P. Müller, A. Nikitin, J. Orphal, V. Perevalov, A. Perrin, D.T. Petkie, A. Predoi-Cross, C.P. Rinsland, J.J. Remedios, M. Rotger, M.A.H. Smith, K. Sung, S. Tashkun, J. Tennyson, R.A. Toth, A.-C. Vandaele, J. Vander Auwera, The 2009 edition of the GEISA spectroscopic database. J. Quant. Spectrosc. Radiat. Transfer 112 (2011) 2395–2445. doi: 10.1016/j.jqsrt. 2011.06.004.

[2] Al. A.A. Azzam, S.N. Yurchenko, J. Tennyson, M.-Al. Martin-Drumel, O. Pirali, Terahertz spectroscopy of hydrogen sulfide, J. Quant. Spectrosc. Radiat. Transfer. 130 (2013) 341–351.

[3] O.V. Naumenko. Private communication (2013).

[4] O.N. Ulenikov, A.B. Malikova, M. Koivusaari, S. Alanko, R. Anttila, High resolution vibrational–rotational spectrum of H_2S in the region of the ν_2 fundamental band, J. Molec.Spectrosc. 176 (1996) 229-235.

[5] J-M. Flaud, C. Camy-Peyret, J.W.C. Johns, The far-infrared spectrum of hydrogen sulphide. The (000) rotational constants of $H_2{}^{32}S$, $H_2{}^{33}S$ and $H_2{}^{34}S$, Can. J. Phys. 61 (1983) 1462-1473.

[6] L.S. Rothman, I.E. Gordon, Y. Babikov, A. Barbe, D. Chris Benner, P.F. Bernath, M. Birk, L. Bizzocchi, V. Boudon, L.R. Brown, A. Campargue, K. Chance, E.A. Cohen, L.H. Coudert, V.M. Devi, B.J. Drouin, A. Fayt, J.-M. Flaud, R.R. Gamache, J.J. Harrison, J.-M. Hartmann, C. Hill, J.T. Hodges, D. Jacquemart, A. Jolly, J. Lamouroux, R.J. Le Roy, G. Li, D.A. Long, O.M. Lyulin, C.J. Mackie, S.T. Massie, S. Mikhailenko, H.S.P. Müller, O.V. Naumenko, A.V. Nikitin, J. Orphal, V. Perevalov, A. Perrin, E.R. Polovtseva, C. Richard, M.A.H. Smith, E. Starikova, K. Sung, S. Tashkun, J. Tennyson, G.C. Toon, Vl.G. Tyuterev, G. Wagner (2013). The HITRAN 2012 molecular spectroscopic database. J. Quant. Spectrosc. Radiat. Transfer Vol. 130, 4–50. doi: 10.1016/j.jqsrt.2013.07.002.

[7] Y. Ding, O.V. Naumenko, S.-M. Hu, Q. Zhu, E. Bertseva, A. Campargue, The absorption spectrum of H_2S between 9540 and 10000 cm^{-1} by intracavity laser absorption spectroscopy with a vertical external cavity surface emitting laser, J. Molec. Spectrosc. 217 (2003) 222-223.

CH_3Br (molecule 43)

In GEISA-2015, the complete line list of CH_3Br present in GEISA-2011 has been updated by adding the temperature dependence of both self- and N_2-broadening coefficients for all transitions. Measurements performed for numerous transitions in the strong ν_6 band led to a *J*-dependent model of the temperature exponents n_{self} and n_{N2} **[1]**. The polynomial expansions of the temperature exponents n_{self} and n_{N2} (see equations **[**4**]** and **[**5**]** from Ref. **[1]** respectively) were used

to update all transitions in GEISA neglecting both the *K*-rotational dependence and the vibrational dependence. The approximation $n_{air} \sim n_{N2}$ was made for the temperature-dependence coefficient *n* of the air-broadening half-width.

Reference

[1] D. Jacquemart, H. Tran, Temperature dependence of self- and N_2-broadening coefficients for CH_3Br in the 10-μm spectral region, J. Quant. Spectrosc. Radiat. Transfer. 109 (2008) 569–579.

HNC (molecule 46)

Barber et al. **[1]** actually performed a combined analysis of the HCN/HNC system. For this they used Mellau's empirical HNC energy levels **[2,3]**, and the line intensities of Harris et al. **[4]**. The resulting GEISA-2015 296 K HNC line list contains 75,554 transitions against 5619 in GEISA-2011.

References

[1] R.J. Barber, J. Strange, C. Hill, O.L. Polyansky, G. Mellau, S.N. Yurchenko and J. Tennyson, ExoMol Molecular linelists: III An improved hot rotation-vibration line list for HCN and HNC, Mon. Not. Roy. Astron. Soc. 437 (2014) 1828-1835.

[2] G.C. Mellau, Complete experimental rovibrational eigenenergies of HNC up to 3743cm^{-1} above the ground state, J. Chem. Phys., 133. (2010) 164303.

[3] G.C. Mellau, Highly excited rovibrational states of HNC, J. Molec. Spectrosc. 269 (2011) 77-85.

[4] G.J. Harris, J. Tennyson, B.M. Kaminsky, Ya.V. Pavlenko, and H.R.A. Jones, Improved HCN/HNC linelist, model atmospheres synthetic spectra for WZ Cas, Mon. Not. R. astron. Soc. 367 (2006) 400-406.

HDO (molecule 51)

As already pointed out, for atmospheric applications, H_2O and HDO need to be taken into account separately in radiative transfer models (as different vertical concentrations may occur), This, combined with their different symmetry properties, led to decide to consider HDO as an independent molecular species in GEISA-2015. The 2015 update of the HDO entries has been very

significant, giving a total of 63,641 lines, against 12,766 in GEISA-2011. This increase is mainly due to the inclusion of empirical line lists in GEISA-2015 HDO update.

Two isotopologues have been involved in the update: i.e.: $HD^{16}O$ and $HD^{18}O$, as summarized in Table1. No update occurred for $HD^{17}O$ which retains the 175 entries from GEISA-2011; for each species are provided, in columns 2 to 7 respectively: its line list spectral range minimum and maximum wave number (cm^{-1}), the number of transitions, the mean and the maximum of the line intensities (cm $molecule^{-1}$ at 296 K), and the origin of the data.

Table 1
General overview of the HDO update in GEISA-2015

Isot. ID	**Wavenb. min (cm^{-1})**	**Wavenb. max (cm^{-1})**	**#lines**	**Moy. I (cm $molec^{-1}$) at 296 K**	**Max. I (cm $molec^{-1}$) at 296 K**	**Origin**
$HD^{16}O$ 162	0.007002	17080.098180	53706	$3.175x10^{-25}$	$2.700\ x10^{-22}$	IAO LIPhy
$HD^{17}O$ 172	1234.234730	1598.765470	175	$4.075x10^{-27}$	$9.319\ x10^{-27}$	GEISA-2011
$HD^{18}O$ 182	0.196882	8748.128100	9760	$3.694x10^{-27}$	$5.646\ x10^{-25}$	IAO LIPhy

The new $HD^{16}O$ set, in GEISA-2015, consists of 53,706 transitions in the 0 - 17104 cm^{-1} spectral region, compared to 11,932 transitions between 0 and 13900 cm^{-1} in GEISA-2011. The difference in contents, between the previous, GEISA-2011, and new enlarged GEISA-2015 $HD^{16}O$ line lists, is illustrated on Fig. 1 and Fig.2. Coincident transitions in GEISA-2011 and GEISA-2015 are plotted with the same (blue) color on both figures. In the new GEISA-2015 version, the previous data, in the 5850-7921 cm^{-1} region, are replaced by those from the exhaustive list of Mikhaïlenko et al. **[1]**. This list includes both observed lines from Refs. **[2-4]** (2730 lines) and 6095 empirical lines based on works on potential energy surface and dipole moment surface **[5-7]** and on the IUPAC TG energy levels **[8]**.

Inaccurate positions of about 900 lines of $HD^{16}O$ between 5 and 7916 cm^{-1}, from GEISA-2011, were replaced with those from the empirical list generated in Ref. **[9]**.

Obviously, the new $HD^{16}O$ list is about three times larger than the GEISA-2011 version. In particular, the majority of the $HD^{16}O$ lines above 7500 cm^{-1} are new. In the near infrared spectral

region, an advantage of this list is that $HD^{16}O$ line parameters are provided in the 1.6 and 1.28 μm atmospheric windows where this minor isotopologue in natural abundance has a major contribution.

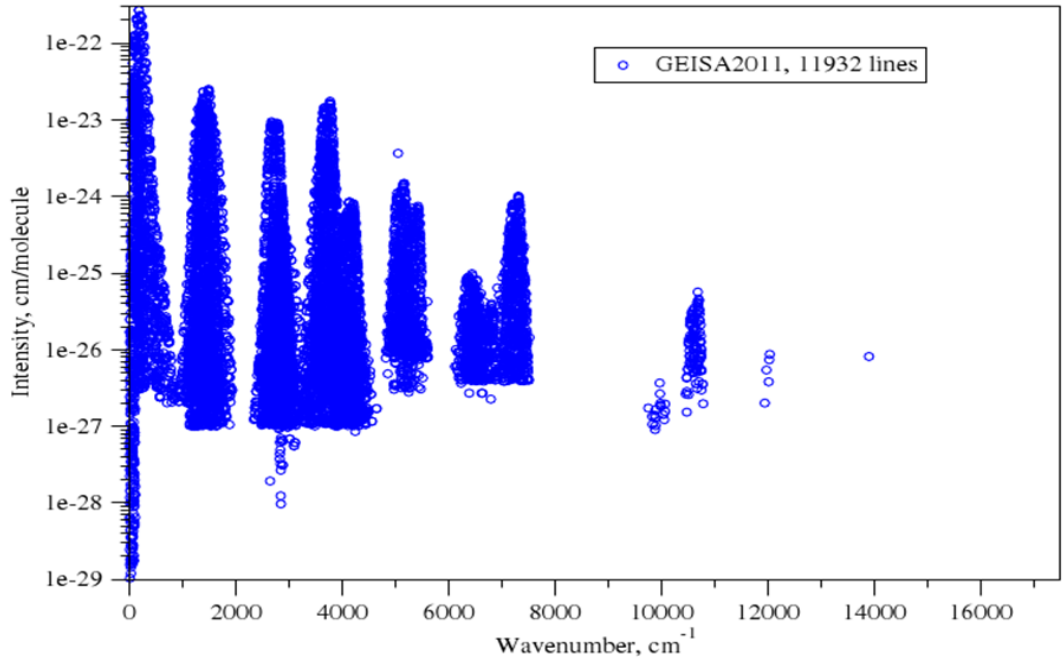

Fig. 1. $HD^{16}O$ transitions in the GEISA-2011 database.

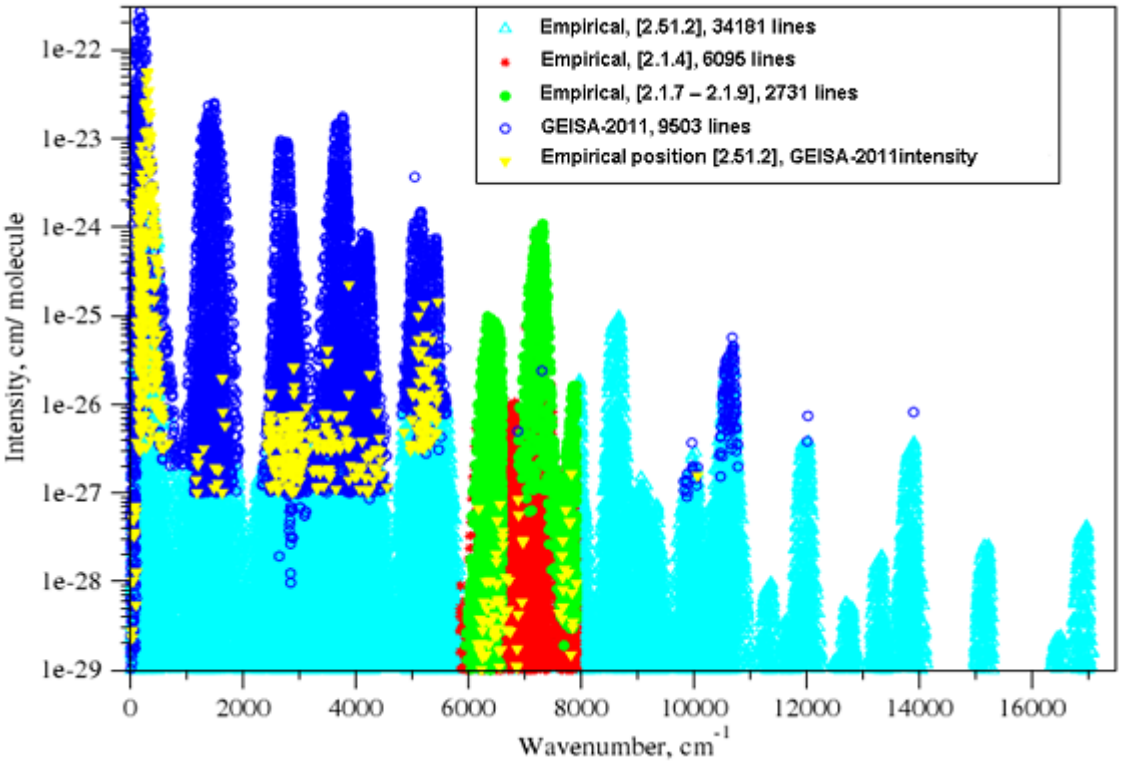

Fig. 2. Composition of the $HD^{16}O$ transition set in GEISA-2015.

An important update has also been performed in GEISA-2015 for the $HD^{18}O$ isotopologue. The $HD^{18}O$ linelist includes now 9760 transitions in the 0.196882-8748.128100 cm^{-1} spectral range (compared to 659 transitions previously). The new $HD^{18}O$ line list was constructed in the following way: The highly accurate experimental microwave and far infrared lines of Refs. **[10-12]**, 204 in total, are used in 0-200 cm^{-1} region. Positions of other lines are derived from the experimental energy levels obtained in Refs. **[11,13-15],**, while the intensities represent variational values based on Partridge and Schwenke potential and dipole moment surfaces **[5-7]**. $HD^{18}O$ line parameters for near infrared are included in GEISA region for the first time.

Fig. 3 presents a comparison between HITRAN-2012 and GEISA-2015, showing the importance of the added HDO data in GEISA-2015; HDO strongly impacts the absorption in the 1.6 µm and 1.28 µm atmospheric windows.

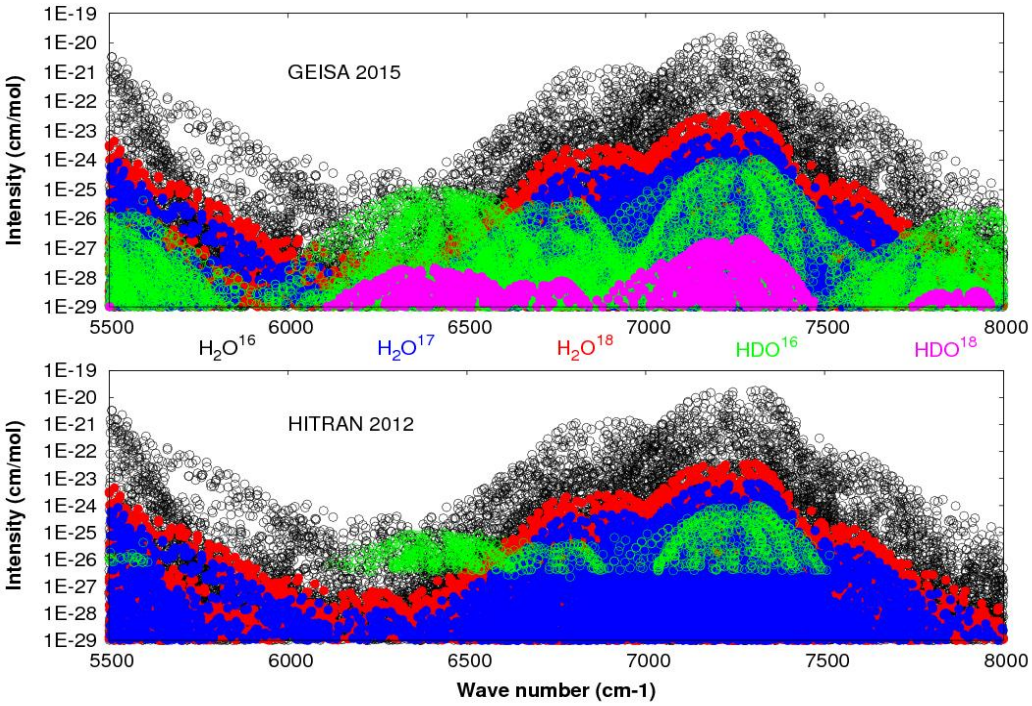

Fig.3. Illustration of the difference between GEISA-2015 and HITRAN-2012 water vapor archives and of the importance of the impact of HDO in the 1.6 and 1.28 µm atmospheric windows. The contribution of the different isotopologues is highlighted ($H_2{}^{16}O$ -black, $H_2{}^{17}O$ -blue, $H_2{}^{18}O$ -red, $HD^{16}O$ -green, $HD^{18}O$ -pink).

For the deuterated isotopologues, $HD^{16}O$, $HD^{18}O$, $HD^{17}O$, the line shape parameters i.e.: the air-broadened half-widths, γ_{air}, its temperature dependence, n_{air}, the air-induced line shifts, δ_{air}, and the self-broadened half-widths, γ_{self}, an algorithm similar to that used for the

three most abundant water isotopologues, $H_2{}^{16}O$, $H_2{}^{18}O$, $H_2{}^{17}O$ was developed using the measurement database of Gamache and Hartmann **[16].**

References

[**1**] S. Mikhailenko, D. Mondelain, S. Kassi, A. Campargue, An accurate and complete empirical line list for water vapor between 5850 and 7920 cm^{-1}, J. Quant. Spectrosc. Radiat. Trans. 140 (2014) 48-57.

[**2**] S. Mikhailenko, S. Kassi, L. Wang, A. Campargue, The absorption spectrum of water in the 1.25 μm transparency window (7408 – 7920 cm^{-1}), J. Mol. Spectrosc. 269 (2011) 92-103.

[**3**] O. Leshchishina, S. Mikhailenko, D. Mondelain, S. Kassi, A. Campargue, CRDS of water vapor at 0.1 Torr between 6886 and 7406 cm^{-1}, J. Quant. Spectrosc. Radiat. Trans. 113 (2012) 2155-2166.

[**4**] O. Leshchishina, S. Mikhailenko, D. Mondelain, S. Kassi, A. Campargue, An improved line list for water vapor in the 1.5 μm transparency window by highly sensitive CRDS between 5852 and 6607 cm^{-1}, J. Quant. Spectrosc. Radiat. Trans. 130 (2013) 69-80.

[**5**] http://spectra.iao.ru

[**6**] D.W. Schwenke, H. Partridge, Convergence testing of the analytic representation of an ab initio dipole moment function for water: Improved fitting yields improved intensities, J. Chem. Phys. 113 (2000) 6592-6597.

[**7**] H. Partridge, D.W. Schwenke, The determination of an accurate isotope dependent potential energy surface for water from extensive *ab initio* calculations and experimental data, J. Chem. Phys. 106 (1997) 4618-4639.

[**8**] J. Tennyson, P.F. Bernath, L.R. Brown. A. Campargue, M.R. Carleer, A.G. Császár, et al., IUPAC critical evaluation of the rotational-vibrational spectra of water vapor. Part II. Energy levels and transition wavenumbers for $HD^{16}O$, $HD^{17}O$, and $HD^{18}O$, J. Quant. Spectrosc. Radiat. Transfer 110 (2010) 2160-2184.

[**9**] N.N. Lavrentieva, B.A. Voronin, O.V. Naumenko, A.D. Bykov, A.A. Fedorova, Line list of $HD^{16}O$ for study of atmosphere of terrestrial planets (Earth, Venus and Mars), Icarus, 236 (2014) 38-47.

[**10**] J.W.C. Johns, High-resolution far-infrared (20–350 cm^{-1}) spectra of several isotopic species of H_2O, J. Opt. Soc. Am. B 2 (1985) 1340-1354.

[**11**] A.-W. Liu, K.-F. Song, H.-Y. Ni, S.-M. Hu, O.V. Naumenko, I.A. Vasilenko, S.N. Mikhailenko, (000) and (010) energy levels of the $HD^{18}O$ and $D_2{}^{18}O$ molecules from analysis of their υ_2 bands, J. Molec. Spectrosc. 265 (2011) 26-38.

[**12**] G. Steenbeckeliers, Private communication (July 1971). These data have been reproduced by Lovas at F.J. Lovas, Microwave spectral Tables. II. Triatomic molecules, J. Phys. Chem. Ref. Data, 7 (1978) 1445-1750

[**13**] A.-W. Liu, J.-H. Du, K.-F. Song, L. Wang, L. Wan, S.-M. Hu, High-resolution Fourier-transform spectroscopy of ^{18}O-enriched water molecule in the 1080 – 7800 cm^{-1} region, J. Mol. Spectrosc. 237 (2006) 149-162.

[**14**] I.A. Vasilenko, E.R. Polovtseva, O.V. Naumenko, A.P. Scherbakov, A.D. Bykov, A.-W. Liu. K.-F. Song, H.-Y. Ni, S.-M. Hu, Fourier transform absorption spectrum of deuterated water vapor enriched by ^{18}O between 2080 and 4600 cm^{-1}, J. Quant. Spectrosc. Radiat. Transfer, to be submitted (2015).

[**15**] S.N. Mikhailenko, O.V. Naumenko, A.V. Nikitin, I.A. Vasilenko, A.-W. Liu, K.-F. Song, H.-Y. Ni, S.-M. Hu, Absorption spectrum of deuterated water vapor enriched by ^{18}O between 6000 and 9200 cm^{-1}, J. Quant. Spectrosc. Radiat. Transfer, 113 (2012) 653-669.

[**16**] R.R. Gamache, J-M. Hartmann, An intercomparison of measured pressur x 10-broadening and pressur x 10-shifting parameters of water vapor, Can. J. Chem.; 82 (2004) 1013-1027.

SO_3 (molecule 52, new in GEISA-2015)

SO_3 was absent for previous editions of GEISA in part because there were no absolute intensity measurements available for this molecules that placed severe limitations on the use of its infrared spectrum for remote sensing applications. However, thanks to the availability of a computed, complete, *ab-initio*, room-temperature line list by Underwood et al. **[294]**, SO_3 has been implemented as a new molecule in GEISA-2015, involving. 10,881 lines of the main $^{32}S^{16}O_3$ isotopologue, in the spectral range 0.477672-2824.347247 cm^{-1}.

In the absence of no measurements or calculations for the line-shape parameters, usual default were chosen, i.e.:

HWHM γ_{air} = 0.0700 $cm^{-1}atm^{-1}$ at 296 K

HWHM self γ_{self} = 0.100 $cm^{-1}atm^{-1}$

Temperature-dependence coefficient *n* of the air broadening half width n_{air} =0.700

The GEISA standard default value has been attributed to the air pressure induced shift of the line transition: δ_{air} = 0.000000 cm^{-1} atm^{-1}.

Reference

[1] D.S. Underwood, J. Tennyson, S.N. Yurchenko, An ab initio variationally computed room-temperature line list for SO_3, Phys. Chem. Chem. Phys. 15(2013) 10118-10125.

1 Appendix A. List of acronyms

4A	Atlas Automatisé des Absorptions Atmosphériques; Automatized Atmospheric Absorption Atlas
4A/OP	4A/OPerational release
ACE	Atmospheric Chemistry Experiment
AERIS	Atmosphere and service data pole (CNES, CNRS), France
AFGL	Air Force Geophysics Laboratory
AIRS	Atmospheric Infrared Sounder
ARIA	Aerosol Refractive Index Archive/University of Oxford (UK)
ARA/ABC(t)	Atmospheric Radiation Analysis/Atmosphère-Biosphère-Climat (télédétection)
BEAMCAT	BErnese Atmospheric Meta Catalog Access Tool
CAL/VAL	Calibration/Validation
CAS RN	Chemical Abstract Service Registry Number
CDMS	Cologne Database for Molecular Spectroscopy
CDSD	Carbon Dioxide Spectroscopic Databank
CIRS	Composite InfraRed Spectrometer
CNRS	Centre National de la Recherche Scientifique (France)
CNES	Centre National d'Etudes Spatiales (France)
CRB	Complex Robert-Bonamy
CRDS	Cavity ring-down spectroscopy
DAS	Differential laser Absorption Spectroscopy
DMS	Dipole Moment Surface
CW-CEAS	Continuous Wave-Cavity Absorption Spectroscopy
CW-CRDS	Continuous Wave-Cavity Ring Down Spectroscopy
ENVISAT	ENVIronmental SATellite
ESPRI	Ensemble de Services pour la Recherche à l'IPSL (Centre for Data and Services belonging to IPSL), CNRS, France
EUMETSAT	European Organisation for the Exploitation of Meteorological Satellites
FTIR	Fourier Transformed InfraRed spectroscopy
FTS	Fourier Transform Spectrometer
GEISA	Gestion et Etude des Informations Spectroscopiques Atmosphériques; Management and study of Atmospheric Spectroscopic Information
GOSAT	Greenhouse Observing SATellite project
GS	Ground State
GSMA	Groupe de Spectroscopie Moléculaire et Atmosphérique (France)
GWP	Global Warming Potential
HITRAN	HIgh-resolution TRANsmission molecular absorption database
HULIS	HUmic-LIke Substances
HWHM	Half Width at Half Maximum
ICLAS	Intra Cavity Laser Absorption Spectroscopy
IASI	Infrared Atmospheric Sounder Interferometer
IASI/NG	Infrared Atmospheric Sounder Interferometer/New Generation
ICB	Institut Carnot de Bourgogne
ID	Identification code
INSU	Institut National des Sciences de l'Univers (France)
IPSL	Institut Pierre Simon Laplace

IAO	Institute of Atmospheric Optics (Russia)
IR	InfraRed
ISSWG	IASI Sounding Science Working Group
IUPAC	International Union of Pure and Applied Chemistry
IUPAC TG	IUPAC Task Group
JPL	Jet Propulsion Laboratory (USA)
KIT	Institute for Meteorology and Climate Research Centre Karlsruhe, (Germany)
LIPhy	Laboratoire Interdisciplinaire de Physique (France)
LISA	Laboratoire Inter-Universitaire des Systèmes Atmosphériques (France)
LMD	Laboratoire de Météorologie Dynamique (France)
Non-LTE	non-Local Thermodynamic Equilibrium
MARVEL	Measured Active Rotational-Vibrational
MCRB	Modified Complex Robert-Bonamy
MERLIN	Methane Remote Sensing Lidar Mission
MIPAS	Michelson Interferometer for Passive Atmospheric Sounding
Metop	Meteorological operational satellite
MOPD	Maximum Optical Path Difference
MWIR	Mid-wavelength infrared
NASA	National Aeronautics and Space Administration (USA)
NCAR	National Center for Atmospheric research (USA)
NIR	Near-InfraRed
PAN	PeroxyAcetyl Nitrate
PSC	Polar Sratospheric Cloud
PES	Potential Energy Surface
RTM	Radiative Transfer Modeling
SCIAMACHY	SCanning Imaging Absorption spectroMeter for Atmospheric ChartograpHY
SRON	Netherlands Institute for Space Research, The Netherlands
S&MPO	Spectroscopy & molecular properties of Ozone
UCC	University College Cork, Ireland
UCL	University College, London (UK)
UV	Ultra Violet
VAMDC	Virtual Atomic and Molecular Data Centre
VECSEL	Vertical External Cavity Surface Emitting Laser
VOC	Volatile organic compounds
VTT	Voronin, Tolchenov, Tennyson
WKLMC	Wang, Kassi, Leshchishina, Mondelain, Campargue
WN	Wave Number (cm^{-1})

2 Appendix C. Molecules and isotopologues in GEISA-2015

Description of molecule and isotopologue codes in GEISA-2015 are given in Table 16. The molecule names and associated codes are in the two first columns; for each molecule, the isotopologue codes and the corresponding detailed formula are in columns 3 and 4 respectively. New molecules are in red and new isotopologues are in purple.

Table 16 Description of molecule and isotopologue codes in GEISA-2015

Molecule	Molecule Code	Isotope Code	Formula
H_2O	1	161	$H^{16}OH$
		171	$H^{17}OH$
		181	$H^{18}OH$
		262	**$D_2{}^{16}O$**
		282	**$D_2{}^{18}O$**
CO_2	2	626	$^{16}O^{12}C^{16}O$
		636	$^{16}O^{13}C^{16}O$
		628	$^{16}O^{12}C^{18}O$
		627	$^{16}O^{12}C^{17}O$
		638	$^{16}O^{13}C^{18}O$
		637	$^{16}O^{13}C^{17}O$
		828	$^{18}O^{12}C^{18}O$
		728	$^{17}O^{12}C^{18}O$
		727	**$^{17}O^{12}C^{17}O$**
		838	$^{18}O^{13}C^{18}O$
		738	**$^{17}O^{13}C^{18}O$**
		737	**$^{17}O^{13}C^{17}O$**
O_3	3	666	$^{16}O^{16}O^{16}O$
		668	$^{16}O^{16}O^{18}O$
		686	$^{16}O^{18}O^{16}O$
		667	$^{16}O^{16}O^{17}O$
		676	$^{16}O^{17}O^{16}O$
N_2O	4	446	$^{14}N^{14}N^{16}O$
		447	$^{14}N^{14}N^{17}O$
		448	$^{14}N^{14}N^{18}O$
		456	$^{14}N^{15}N^{16}O$
		546	$^{15}N^{14}N^{16}O$
		458	$^{14}N^{14}N^{18}O$
		548	$^{15}N^{14}N^{18}O$
		556	$^{15}N^{15}N^{16}O$

Molecule	Molecule Code	Isotope Code	Formula
CO	5	26	$^{12}C^{16}O$
		27	$^{12}C^{17}O$
		28	$^{12}C^{18}O$
		36	$^{13}C^{16}O$
		37	$^{13}C^{17}O$
		38	$^{13}C^{18}O$
CH_4	6	211	$^{12}CH_4$
		311	$^{13}CH_4$
O_2	7	66	$^{16}O^{16}O$
		67	$^{16}O^{17}O$
		68	$^{16}O^{18}O$
NO	8	46	$^{14}N^{16}O$
		48	$^{14}N^{18}O$
		56	$^{15}N^{16}O$
SO_2	9	626	$^{32}S^{16}O_2$
		646	$^{34}S^{16}O_2$
NO_2	10	646	$^{14}N^{16}O_2$
NH_3	11	411	$^{14}NH_3$
		511	$^{15}NH_3$
PH_3	12	131	$^{31}PH_3$
HNO_3	13	146	$H^{14}N^{16}O$
		156	$H^{15}N^{16}O$
OH	14	61	^{16}OH
		62	^{16}OD
		81	^{18}OH
HF	15	19	$H^{19}F$
HCl	16	15	$H^{35}Cl$
		17	$H^{37}Cl$
HBr	17	11	$H^{81}Br$
		19	$H^{79}Br$
HI	18	17	$H^{127}I$
ClO	19	56	$^{35}Cl^{16}O$
		76	$^{37}Cl^{16}O$
OCS	20	622	$^{16}O^{12}C^{32}S$
		623	$^{16}O^{12}C^{33}S$
		624	$^{16}O^{12}C^{34}S$
		632	$^{16}O^{13}C^{32}S$
		634	$^{16}O^{13}C^{34}S$
		822	$^{18}O^{12}C^{32}S$
H_2CO	21	126	$H_2{}^{12}C^{16}O$
		128	$H_2{}^{12}C^{18}O$
		136	$H_2{}^{13}C^{16}O$
		226	$^{12}C_2H_6$

Molecule	Molecule Code	Isotope Code	Formula
C_2H_6	22	236	$^{12}C^{13}CH_6$
CH_3D	23	212	$^{12}CH_3D$
		312	$^{13}CH_3D$
C_2H_2	24	221	$^{12}C_2H_2$
		231	$^{12}C^{13}CH_2$
C_2H_4	25	211	$^{12}C_2H_4$
		311	$^{12}C^{13}CH_4$
GeH_4	26	411	$^{74}GeH_4$
HCN	27	124	$H^{12}C^{14}N$
		125	$H^{13}C^{15}N$
		134	$H^{13}C^{14}N$
		224	$D^{12}C^{14}N$
C_3H_8	28	221	$^{12}C_3H_8$
C_2N_2	29	224	$^{12}C_2{}^{14}N_2$
C_4H_2	30	211	$^{12}C_4H_2$
HC_3N	31	124	$H^{12}C_3{}^{14}N$
HOCl	32	165	$H^{16}O^{35}Cl$
		167	$H^{16}O^{37}Cl$
N_2	33	44	$^{14}N^{14}N$
CH_3Cl	34	215	$^{12}CH_3{}^{35}Cl$
		217	$^{12}CH_3{}^{37}Cl$
H_2O_2	35	166	$H_2{}^{16}O^{16}O$
H_2S	36	121	$H_2{}^{32}S$
		131	$H_2{}^{33}S$
		141	$H_2{}^{34}S$
HCOOH	37	261	$H^{12}C^{16}O^{16}OH$
COF_2	38	269	$^{12}C^{16}O^{19}F_2$
SF_6	39	29	$^{32}S^{19}F_6$
C_3H_4	40	341	$^{12}C_3H_6$
HO_2	41	166	$H^{16}O_2$
$ClONO_2$	42	564	$^{15}Cl^{16}O^{14}N^{16}O_2$
		764	$^{17}Cl^{16}O^{14}N^{16}O_2$
CH_3Br	43	79	$^{12}CH_3{}^{79}Br$
		81	$^{12}CH_3{}^{81}Br$
CH_3OH	44	216	$^{12}CH_3{}^{16}OH$
NO+	45	46	$^{14}N^{16}O+$
HNC	46	142	$H^{14}N^{12}C$
C_6H_6	47	266	$^{12}C_6H_6$
C_2HD	48	122	$^{12}C_2HD$
CF_4	49	291	$^{12}C^{15}F_4$
CH_3CN	50	234	$^{12}CH_3{}^{12}C^{14}N$
HDO	**51**	162	$H^{16}OD$
		182	$H^{18}OD$

Molecule	Molecule Code	Isotope Code	Formula
SO_3	**52**	26	$^{32}S^{16}O_3$